AD-A154 592 MULTILAYER CAPACITOR DIELECTRICS PRODUCED FROM METALLO-ORGANIC PRECURSORS(U) PURDUE UNIV LAFAYETTE IN TURNER LAB FOR ELECTROCERAMICS R W VEST ET AL. 1/1

UNCLASSIFIED 29 APR 85 N00014-83-K-0321 F/G 7/1 NL

END

FILMED

DTIC

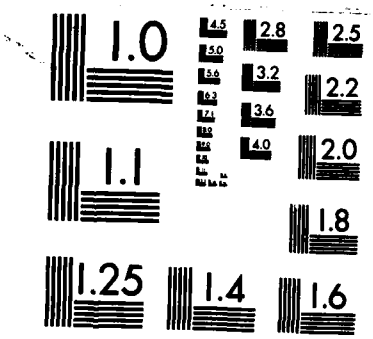

MULTILAYER CAPACITOR DIELECTRICS PRODUCED FROM METALLO-ORGANIC PRECURSORS

R.W. Vest and G.M. Vest

29 April 1985

Annual Report

For the Period 3/1/84 - 2/28/85

Contract No. N00014-83-K-0321

Prepared for: Office of Naval Research

FOREWORD

The research described in this report was conducted under Contract No. N00014-83-K-0321 with the Office of Naval Research under the technical cognizance of Dr. R.C. Pohanka. Research was conducted in the Turner Laboratory for Electroceramics, School of Materials Engineering and School of Electrical Engineering, West Lafayette, Indiana under the direction of R.W. Vest and G.M. Vest. Contributing to the project were Dr. S. Singaram and Messrs. S.K. Muralidhar, R.L. Reed and A.S. Shaikh.

TABLE OF CONTENTS

LIST OF FIGURES

LIST OF TABLES

1. INTRODUCTION

The metallo-organic decomposition (MOD) process for preparing films or powders has a number of advantages over conventional processes. Different types of MOD films have been discussed in various papers and technical reports by the Vests [1-5]. The metallo-organic compounds used in the present study had oxygen as the hetero atom to bond a metal atom to an organic ligand. These compounds were each dissolved in an appropriate solvent and the solutions mixed to achieve the desired stoichiometry. After adjusting the rheology, the formulation was deposited on an appropriate substrate to make a film or contained in a platinum dish to make a powder, and pyrolyzed to yield the inorganic product. Since the mixing of the starting materials is on the molecular level, the inorganic species exist as atoms or molecules in intimate contact immediately after decomposition. This leads to much more rapid formation of compounds and sintering of films, which translates to lower temperature processing of equilibrium phases and films.

This report is divided into three parts. The first details studies of the kinetics of formation of $BaTiO_3^{\eta}$ and $PbTiO_3^{\eta}$ by the MOD process, and demonstrates that the temperatures required are more than 200 C lower than those needed if the finest available powders are used as precursors. The second part of the report describes a study of the defect structure and dielectric properties of $Nd_2^{\eta}O_3^{\eta}$ doped $BaTiO_3^{\eta}$. The use of the MOD process to prepare the various compositions insured the formation of equilibrium phases. The third part of the report discusses preliminary studies of $BaTiO_3^{\eta}$ film formation by the MOD process.

2. KINETICS OF FORMATION OF $BaTiO_3$ and $PbTiO_3$

2.1 General

Conventionally, dielectric materials are produced by solid state reaction between powder precursors. The dielectric properties of such materials are affected to a great extent by the degree of mixing of ingredient materials and impurities introduced through milling. Thus, reproducible dielectric properties are very difficult to achieve by the solid state reaction technique. The MOD technique has great potential of overcoming these difficulties. The firing temperatures involved in the solid state reaction technique are quite high, and special precautions are mandatory in order to prevent PbO loss while preparing $PbTiO_3$. It is possible to prepare compounds involving volatile materials at considerably lower temperature by the MOD process compared to the conventional method.

Barium neodecanoate [$Ba(C_9H_{19}COO)_2$] and titanium dimethoxy dineodecanoate [$(CH_3O)_2Ti(C_9H_{19}COO)_2$]were the precursors used for $BaTiO_3$. Lead acetate trihydrate [$Pb(CH_3COO)_2.3H_2O$] was soluble in titanium dimethoxy dineodecanoate solution in xylene, and those two were used as precursors for $PbTiO_3$. To study the effect of the nature of the precursors, the kinetics of $PbTiO_3$ formation were also studied using lead neodecanoate [$Pb(C_9H_{19}COO)_2$] and titanium dimethoxy dineodecanoate solutions. The kinetics data were fit to appropriate models.

2.2 Experimental

2.2.1 Materials

Selection criteria used for metallo-organic compounds are discussed elsewhere [1,2]. Most of the selected metallo-organic compounds were synthesised in house for better control over experimental variables. However, commercially available lead acetate trihydrate* was used for the $PbTiO_3$ formation studies.

2.2.2 Materials Synthesis

Titanium Dimethoxy Dineodecanoate

Eighty six grams (0.5 moles) of titanium methoxide# was transferred to 1000 ml. flask under an inert atmosphere. Two hundred ml. (1 mole) of 95 % pure neodecanoic acid$ and about 20 ml of spectrographic pure methanol+ were added to the flask without disturbing the inert atmosphere. The reaction mixture was refluxed under the inert atmosphere for at least three hours at 65°C.

A pale yellow viscous liquid was obtained. Methanol from that liquid was removed by vacuum distillation, and the liquid was dissolved in xylene. Traces of unreacted titanium methoxide was filtered out to

* L-33, Fisher Scientific Co., Fair Lawn, NJ 07410.

\# 77137, Alfa Products, 152 Andover Street, Danvers, MA 01923.

$ Neodecanoic Prime, Exxon Chemicals Americas, Houston, TX 77001.

\+ A-408, Fisher Scientific, Fair Lawn, NJ 07410.

obtain a clear pale yellow solution of titanium dimethoxy dineodecanoate in xylene.

Reaction:

$$(CH_3O)_4Ti + 2C_9H_{19}COOH \longrightarrow (C_9H_{19}COO)_2Ti(CH_3O)_2 + 2CH_3OH$$

Barium Neodecanoate

One hundred and fifty g (0.61 moles) of $BaCl_2.2H_2O$** were dissolved in about 300 ml of water. In a 2000 ml beaker, 240 ml (1.2 moles) of neodecanoic acid were neutralized by 75 ml(1.2 moles) of NH_4OH (NH_3 assay: 30 %)##. The solution was stirred for 20-25 minutes. To this ammonium soap solution, the $BaCl_2$ solution was added with vigorous stirring. The white gummy barium soap was formed as a top layer which was dissolved in xylene and was separated from the aqueous layer with the help of a separatory funnel.

Reactions:

$$NH_4OH + C_9H_{19}COOH \longrightarrow C_9H_{19}COONH_4 + H_2O$$
$$2C_9H_{19}COONH_4 + BaCl_2 \longrightarrow 2NH_4Cl + (C_9H_{19}COO)_2Ba$$

Lead Neodecanoate

Two hundred and forty grams (0.73 moles) of $Pb(NO_3)_2$*# were dissolved in about 650-700 ml of water. In a 2000 ml beaker, 280 ml (1.4

** BX60, MCB, Norwood, OH 45212.

A-669 S, Fisher Scientific Co., Fair Lawn, NJ 07410.

moles) of neodecanoic acid(95% purity) were neutralized by 87 ml of NH_4OH (NH_3 assay: 30%). After stirring the solution for 20-25 minutes the $Pb(NO_3)_2$ solution was added with constant stirring. A pale yellow, gummy lead neodecanoate soap settled at the bottom of the flask. It was separated from the aqueous solution and was dissolved in xylene.

Reactions:

$$NH_4OH + C_9H_{19}COOH \longrightarrow C_9H_{19}COONH_4 + H_2O$$

$$2C_9H_{19}COONH_4 + Pb(NO_3)_2 \longrightarrow 2NH_4NO_3 + (C_9H_{19}COO)_2Pb$$

In these preparations, the ammonium soap was purposely used to insure that no impurities such as alkali oxides were introduced in the fired product; unreacted ammonium soap on firing will produce gaseous products such as NH_3, NO_x CO_2 and H_2O.

2.2.3 Compound Characterization

The thermal decomposition behavior of the compounds was studied using thermogravimetric analysis (TGA). The final decomposition products were characterized using an x-ray diffractometer* with Cu-kα radiation. Barium neodecanoate and titanium dimethoxy dineodecanoate decomposed to $BaCO_3$ (witherite) and TiO_2 (anatase) respectively. Both lead acetate and lead neodecanoate produced a mixture of litharge (PbO) and massicot (PbO) on decomposition. Surface areas of the powders obtained at the temperature corresponding to complete decomposition of the

*# LX0159-1, MCB, Norwood, OH 45212.

metallo-organic compounds were measured using the BET method**.

2.2.4 Kinetic Studies

Figures 1-3 show thermograms of xylene solutions of barium neodecanoate, titanium dimethoxy dineodecanoate and an equimolar mixture of barium neodecanoate and titanium dimethoxy dineodecanoate, respectively. The thermogram of the equimolar mixture shows a weight loss around 600-625°C. This weight loss approximately corresponds to the weight loss in the formation of barium titanate from barium carbonate and titanium dioxide. Thus, the kinetics of formation of barium titanate were studied at 600-660°C. Barium neodecanoate and titanium dimethoxy dineodecanoate solutions were mixed in an equimolar proportion. The mixture was heated at a programmed heating rate of 5°C/min. from room temperature to 595, 620 and 660°C, and held at these temperatures for various time periods.

Lead neodecanoate solution in xylene when heated at 5°C/min showed signs of partial evaporation before decomposition. An equimolar solution of lead neodecanoate and titanium dimethoxy dineodecanoate in xylene, and an equimolar solution of lead acetate and titanium dimethoxy dineodecanoate also showed signs of partial evaporation before decomposition when heated at 5°C/min. A lower heating rate gave inhomogeneous decomposition products, where a thin PbO rich layer was observed on the top of the decomposed product. The best results were obtained by adding high boiling point liquids such as ethyl stearate* $[CH_3(CH_2)_{16}CO_2C_2H_5]$ and

* Kristalloflex 4, Siemens Inc., Germany.

** Monosorb, Quantachrome Inc., Greenvale, NY 11548.

Table 2. Comparison of Kinetic Parameters for $BaTiO_3$ Formation Studies.

Precursors	C (sec^{-1})	Q(kJ/mole)
Metallo-organic	4.95×10^8	232
Powder (Amin et al. [7])	1.03×10^6	232

also analyzed. Assuming that the 'K' in the Eq. (3) has a form

$$K=Cexp(-Q/RT) \quad (4)$$

the values of activation energy and the constant C were calculated for the present set of data as well as for Amin et al.'s data. The results of the analyses are presented in Table 2. The values of Q are identical, but the values of C are very different causing the reaction rates to differ. At constant temperature, the same fractional completion of the reaction is achieved with the MOD process in 1/500 of the time required with powder precursors. At constant reaction time for a certain fractional completion, 900°C would be required for powder precursors and 670°C for the MOD process.

The constant 'C' in Eq. (4) is related to the diffusion path lengths. Hence, when using the MOD process the diffusion path lengths are considerably shorter than those in the conventional process, but the basic reaction mechanism remains the same as evidenced by the identical activation energies in Table 2. This is the result of the intimate mixing and finer grain size of the powders formed by the MOD process. Table 3 compares the BET surface areas of the reactants used by Amin et al. [7] with those obtained by the MOD process. The particle sizes of reactants obtained by decomposition of metallo-organic compounds are smaller by factors of 5 to 14 compared to the finest available commercial powders.

Figures 8 and 9 are plots of $-\ln(1-\alpha)$ versus (t) for $PbTiO_3$ formation from lead acetate and titanium dimethoxy dineodecanoate, and lead neodecanoate and titanium dimethoxy dineodecanoate respectively. Table 4

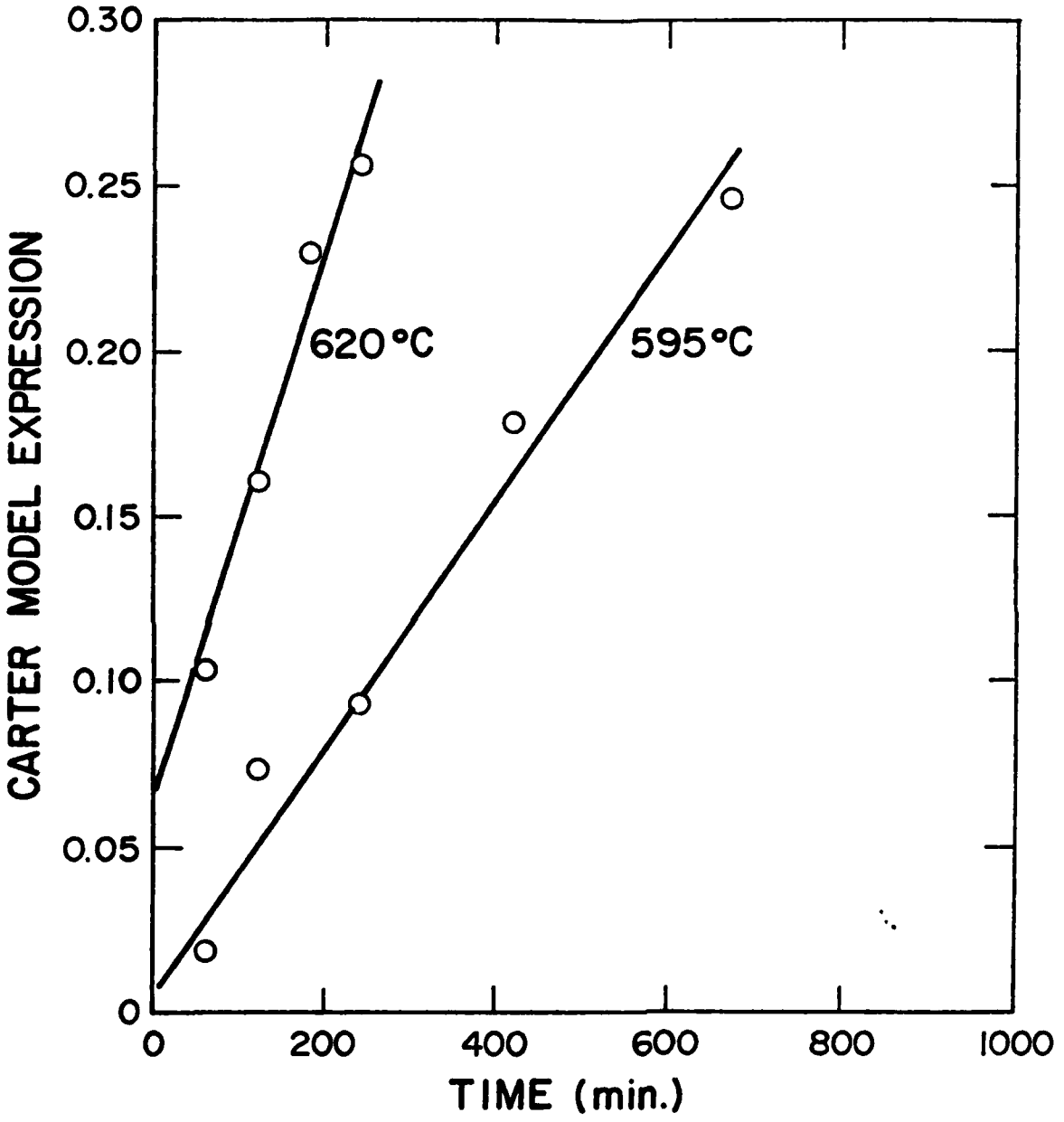

Figure 7. Carter model fit for kinetics of $BaTiO_3$ formation.

cated that Ba_2TiO_4 is formed directly from $BaCO_3$ and TiO_2. Templeton and Pask [10] reported that all the compounds on the phase diagram for BaO-TiO_2 at a certain temperature appear in varying amounts, depending on the rate of diffusion. G. V. Bois et al. [11] suggested that, in a mixture of $BaCO_3$ and the oxides of group IV elements which exhibit polymorphic transitions, the onset temperature of reaction is 0.6 of the absolute polymorphic transition temperature of these oxides. Also, if reaction in these oxides can take place below 900°C only the end product is formed, if the reaction begins above 900°C formation of an intermediate orthocompound is possible. Hence, the $BaCO_3$ and rutile reaction should be slower as compared to the $BaCO_3$ and anatase reaction. Also, the $BaCO_3$-rutile reaction proceeds through formation of Ba_2TiO_4, whereas the $BaCO_3$-anatase reaction directly yields $BaTiO_3$. In the present studies, no peaks for any intermediate phase/phases were detected.

Recently, Amin et al. [7] studied the formation of $BaTiO_3$ from fine powders. They fit the data to the Carter model [12] expression for a diffusion controlled process:

$$\frac{[1 + (Z - 1)\alpha]^{2/3} + (Z - 1)(1 - \alpha)^{2/3} - Z}{(1 - Z)} = \frac{kt}{r^2} = Kt \qquad (3)$$

where Z is the volume of $BaTiO_3$ formed per unit volume of $BaCO_3$ consumed (Amin et al. [7] considered Z as the volume of $BaTiO_3$ formed per unit volume of TiO_2 consumed.), α is the fractional completion of the reaction, after time t, r is the particle size and k is a constant. The $BaTiO_3$ formation data are plotted according to Eq. (3) in Fig. 7. The kinetic data for the reaction between between the fine powders of $BaCO_3$ and TiO_2 (anatase) at 870°C and 910°C reported by Amin et al. [7] were

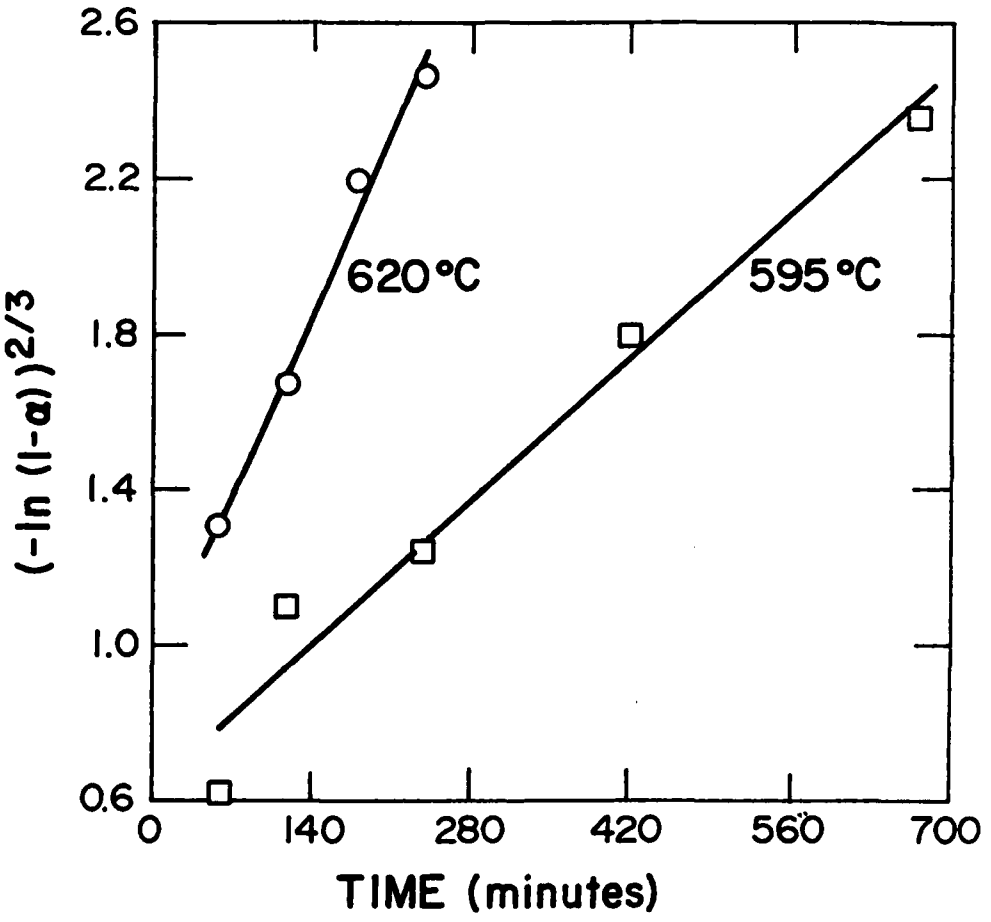

Figure 6. $(-\ln (1-\alpha))^{2/3}$ versus t plot for $BaTiO_3$ formation.

appears that a plot of $\ln(-\ln(1-\alpha))$ versus $\ln(t)$ should give the value of m. However, a $\ln(-\ln(1-\alpha))$ versus $\ln(t)$ plot is very insensitive to the values of m. Hence, an attempt was made to fit the data to all the values of 'm' given in Table 1. In all cases, the best fit was observed for the value of m = 1.5, which corresponds to a diffusion controlled reaction.

Figure 6 is plot of $-\ln(1-\alpha)$ versus (t) for $BaTiO_3$ formation. From the slopes of the lines on Fig. 6, the rate constant (k) in Eq. (1) was found to be 2.64×10^{-3} min^{-1} at $595^{o}C$ and 6.71×10^{-3} min^{-1} at $620^{o}C$. A value m = 1.5 corresponds to a diffusion controlled reaction with zero nucleation rate, that is, nucleation occurs so rapidly that all nucleation sites are exhausted at an early stage in the reaction. The rate constant 'k' in this model can be expressed as[6]

$$k = BD^{m} \qquad (2)$$

where D is the diffusion coefficient and B is a constant related to the shape and number of nuclei. Assuming $D=D_o \exp(-Q/RT)$, and using the values of k, the activation energy for diffusion was found to be 240 kJ/mole.

Solid state reaction between $BaCO_3$ and TiO_2 to form $BaTiO_3$ has been studied extensively and reported to be diffusion controlled [7-10]. However there is no agreement about the way this reaction proceeds. Kubo and Shinriki [8] and Trzebiatowski et al. [9] reported that some $BaTiO_3$ forms first and then Ba_2TiO_4, and finally the orthotitanate combines with TiO_2 to form $BaTiO_3$. According to Kubo and Shinriki [8] Ba_2TiO_4 is produced from $BaTiO_3$ and $BaCO_3$, whereas Trzebiatowski et al. [9] indi-

Table 1. Values of m for Various Nucleation and Three Dimensional Growth Conditions.

Nucleation condition	Phase-boundary controlled	Diffusion controlled
Constant nucleation rate	4	2.5
Zero nucleation rate	3	1.5
Decreasing nucleation rate	3-4	1.5 - 2.5

area under the curve with the help of a computer. The (111) and (021) peaks of $BaCO_3$ lie very close to each other, and at very low concentrations it is hard to resolve these two peaks. Hence, both peaks were chosen for quantitative phase analysis.

X-ray diffraction of the initial decomposition product of an equimolar mixture of lead acetate and titanium dimethoxy dineodecanoate, and lead neodecanoate and titanium dimethoxy dineodecanoate solutions in xylene with methyl/ethyl stearate added showed peaks of litharge (PbO), massicot (PbO) and $PbTiO_3$. Intensities of the (101) peak of litharge, the (111) peak of massicot and the (111) peak of $PbTiO_3$ were chosen for analysis. A standard curve of the ratio of the intensities of the [001] peak of $BaTiO_3$, to the [111] and [021] peaks of $BaCO_3$ versus the ratio of the volume of $BaTiO_3$ to $BaCO_3$ was prepared. Similar curves were prepared for massicot and $PbTiO_3$, and litharge and $PbTiO_3$. The quantitative phase analysis was done using these curves.

2.3 Results and Discussion

A general kinetic expression based on nucleation and growth models is given by [6]

$$\ln\left|\frac{1}{1-\alpha}\right| = kt^m \qquad (1)$$

where α is the fractional completion of the reaction after time t, k is the rate constant, and m is a kinetics parameter, which is function of reaction mechanism, nucleation rate and geometry of nuclei. Table 1 summerizes the values of parameter 'm' for various reaction mechanisms and nucleation conditions for three dimensional growth. From Eq. (1) it

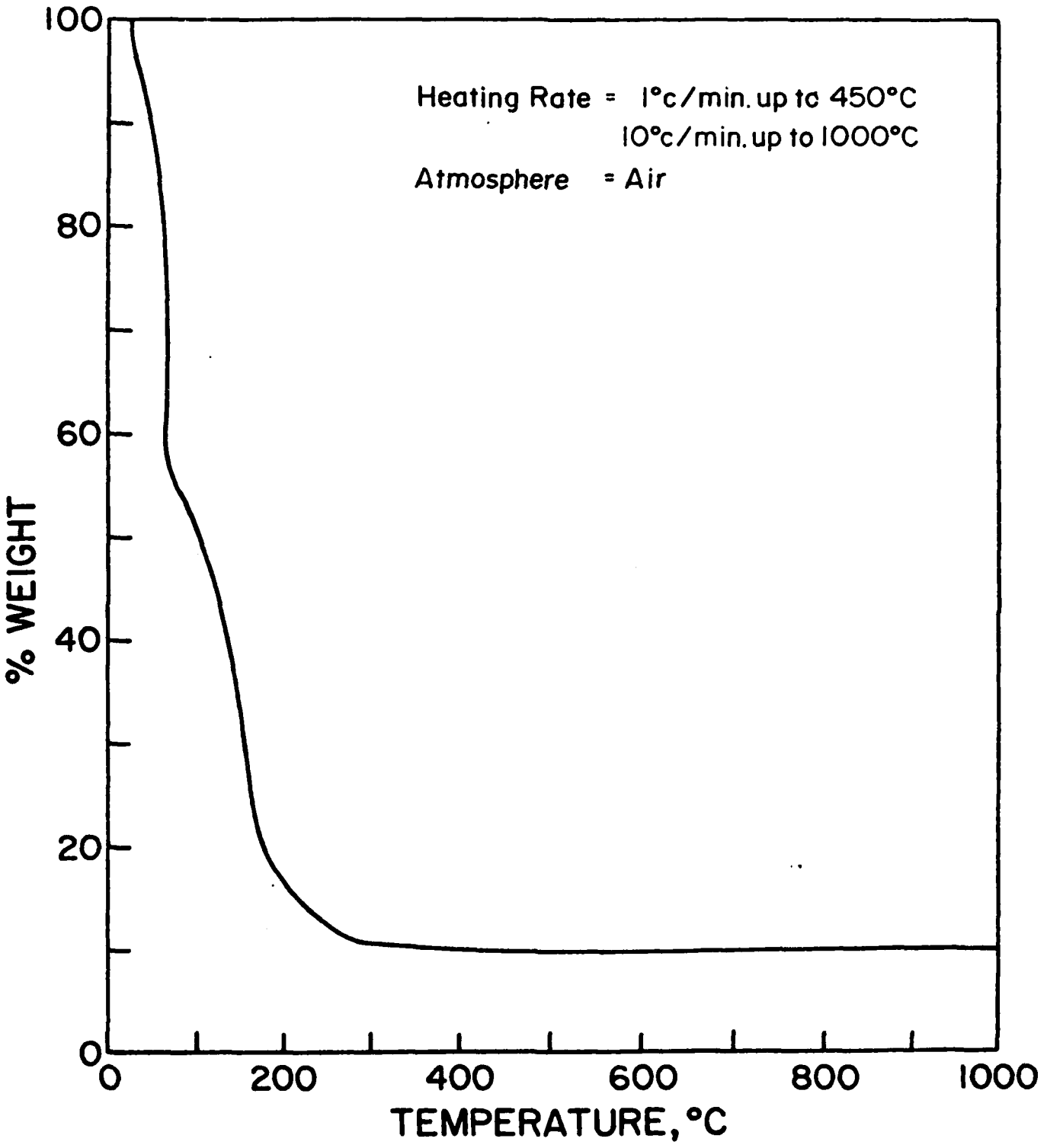

Figure 5. Thermogram of $PbTiO_3$ formulation in xylene.

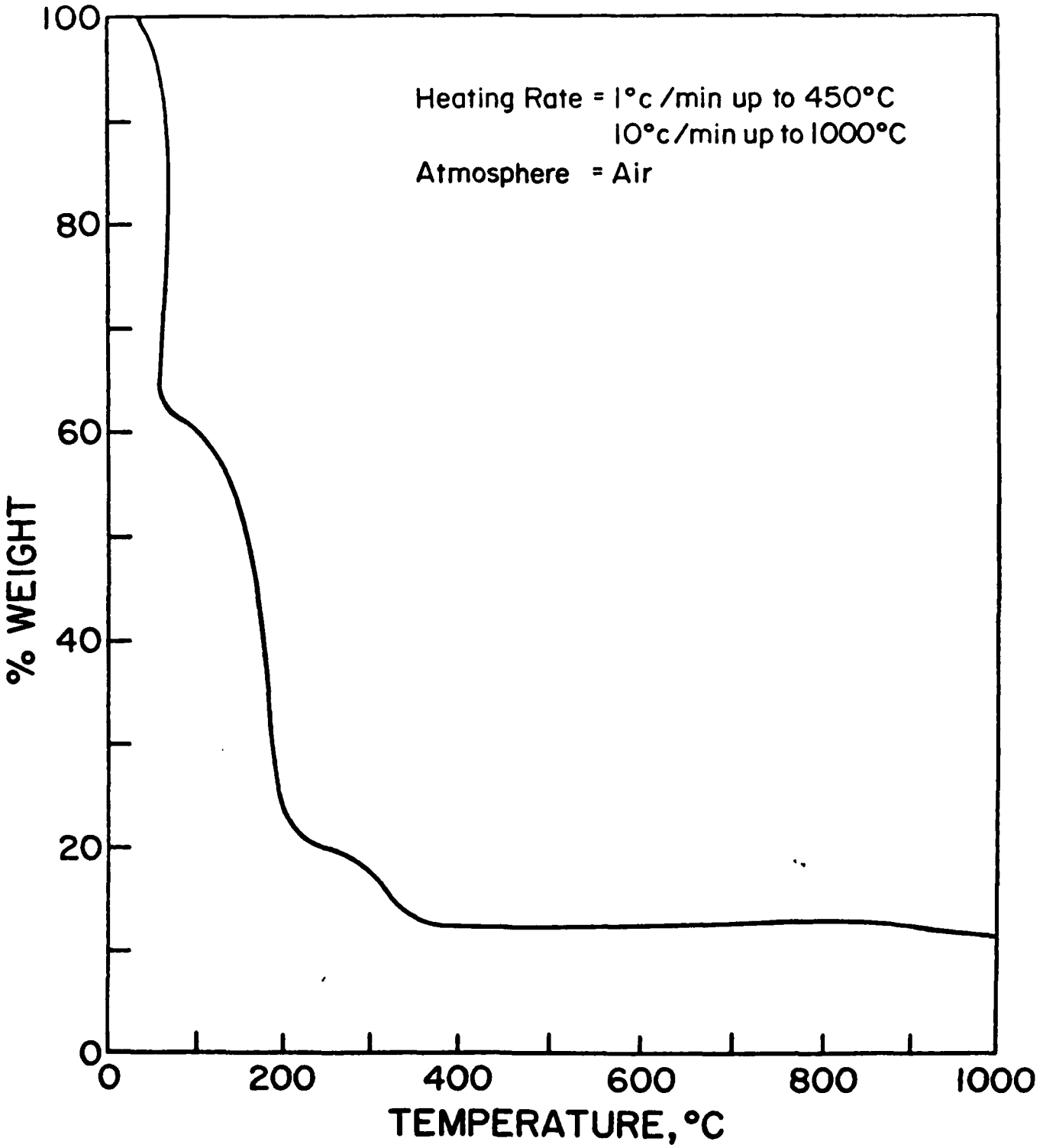

Figure 4. Thermogram of lead neodecanoate solution in xylene with ethyl stearate added.

methyl stearate# [$CH_3(CH_2)_{16}CO_2CH_3$] (b. p. 215°C /15 mm.). Figure 4 is a thermogram of xylene solution of lead neodecanoate with ethyl stearate added to it, and shows weight loss due to PbO evaporation above 800°C. Figure 5 is thermogram of a xylene solution containing an equimolar mixture of lead neodecanoate and titanium dimethoxy dineodecanoate with ethyl stearate added, which shows no weight loss up to 1000°C indicating the formation of $PbTiO_3$ prior to vaporization of PbO. After a few trials, $PbTiO_3$ formation studies were conducted at 450°C, 550°C, 600°C and 650°C. Equimolar amounts of lead acetate and titanium dimethoxy dineodecanoate were mixed together, and methyl stearate was added. The mixture was heated at 100°C/hr to 450°C and held at 450°C for about 50 minutes. The fired product was pulverized and was used for kinetics studies at 450°C, 550°C, 600°C and 650°C. Lead neodecanoate has more tendency for evaporation before decomposition compared to lead acetate. Hence, equimolar amounts of lead neodecanoate and titanium dimethoxy dineodecanoate in xylene and with ethyl stearate added were heated at the lower heating rate of about 60°C/hr to 450°C, and the fired product was pulverized and used for kinetics studies at 450°C, 550°C and 600°C.

X-ray diffraction of the initial decomposition product of the $BaTiO_3$ formulation showed only $BaCO_3$ and $BaTiO_3$ peaks. The particle size of the anatase was too small to give a diffraction pattern. Intensities of the [111] and [021] peaks of $BaCO_3$ and the [001] peak of $BaTiO_3$ were measured by taking electronic counts at angular intervals of 0.025°, fitting the electronic counts to a curve, and measuring the

* M 8,070-9, Aldrich Chem. Inc., Milwaukee, WIS 53233.

22317-4, Aldrich Chem. Inc., Milwaukee, WIS 53233.

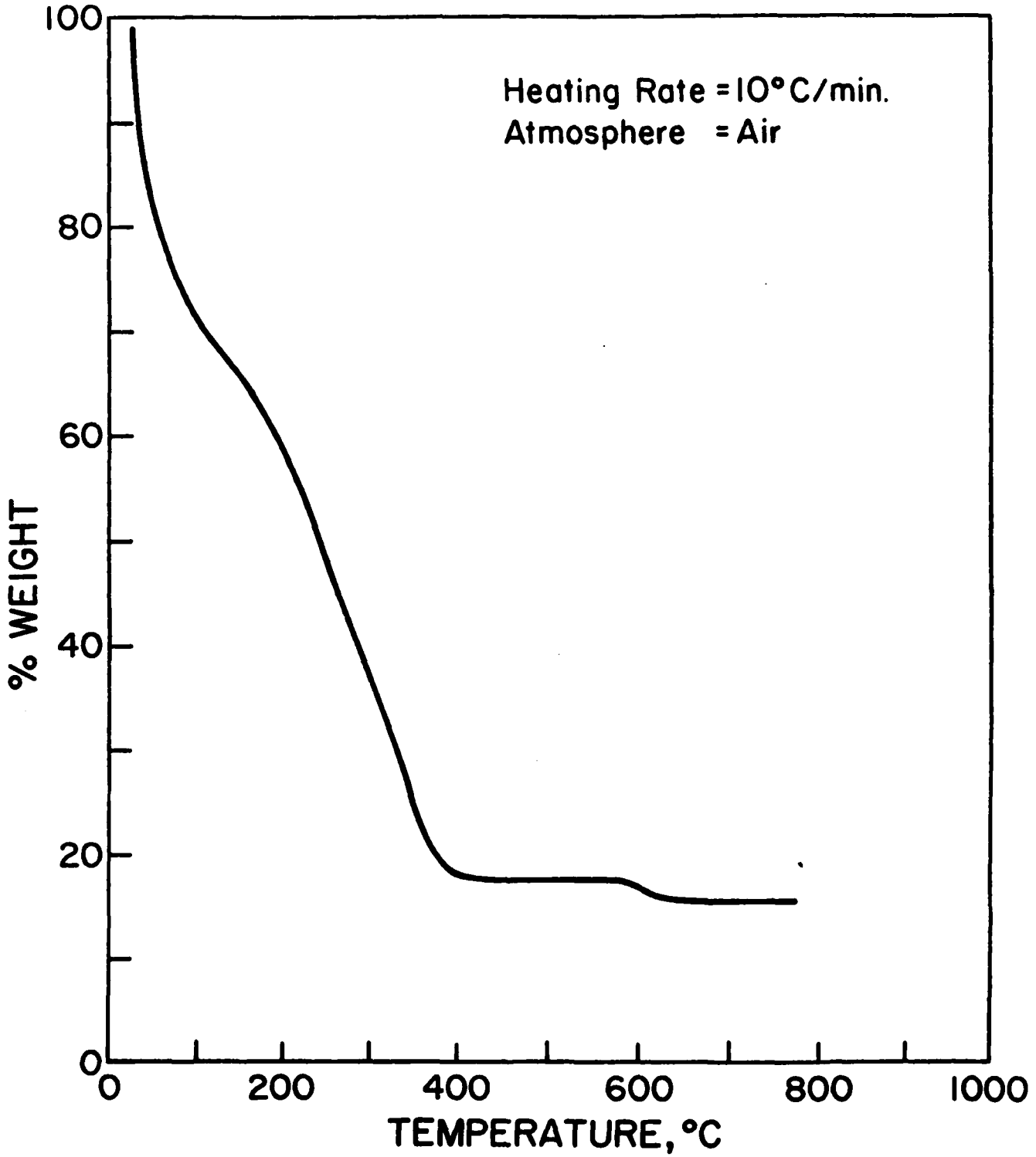

Figure 3. Thermogram of $BaTiO_3$ formulation in xylene.

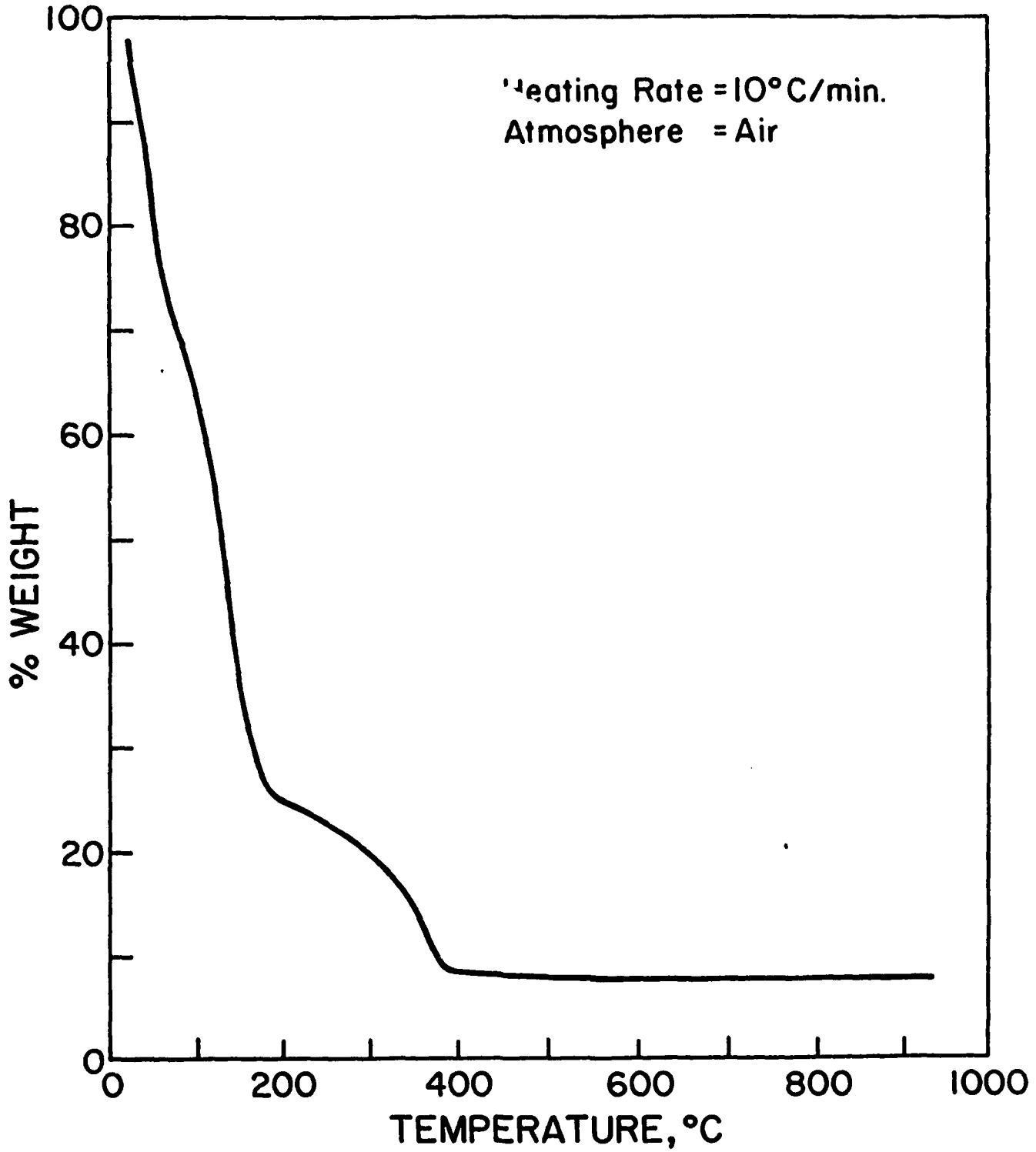

Figure 2. Thermogram of titanium dimethoxy dineodecanoate solution in xylene.

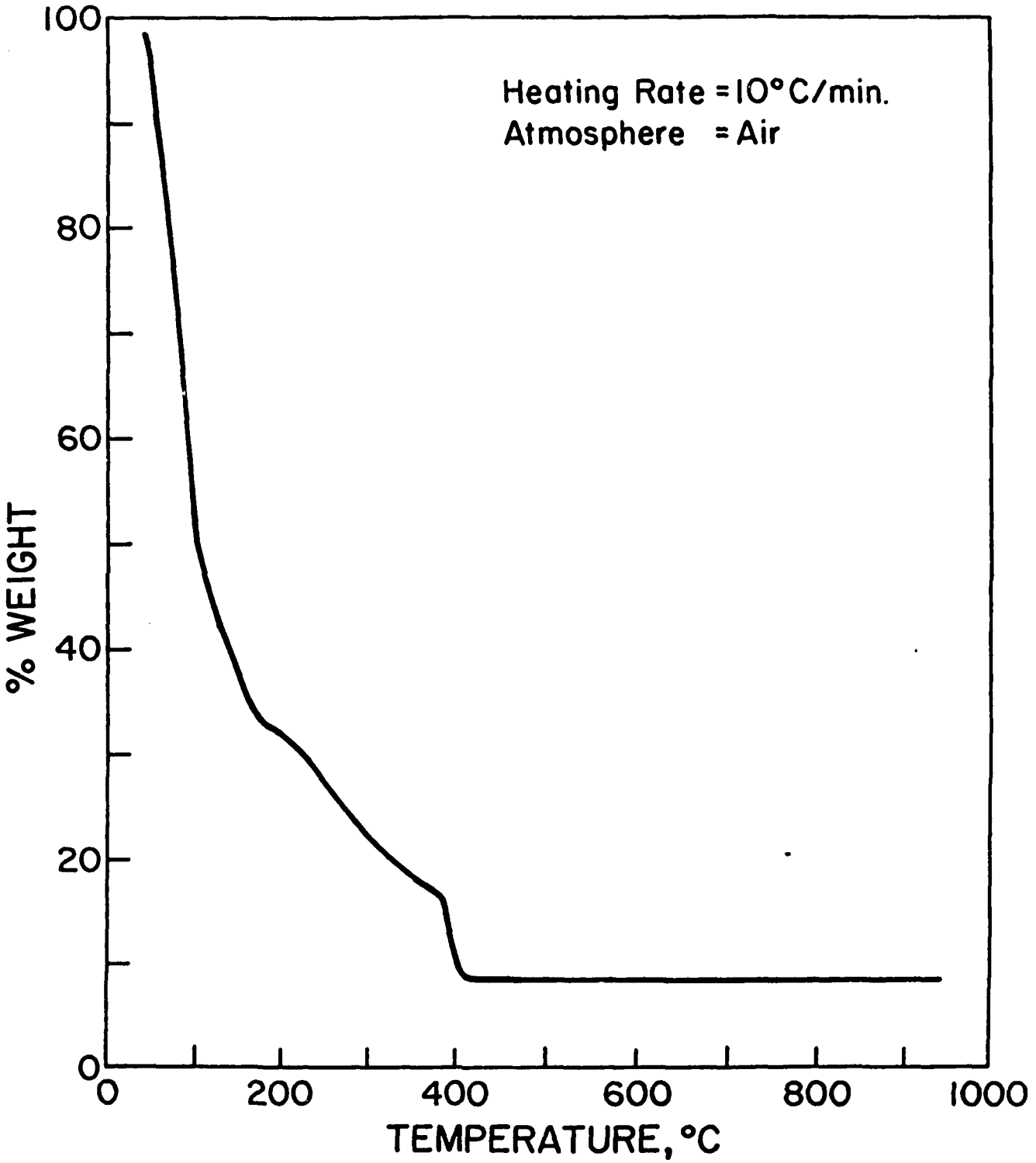

Figure 1. Thermogram of barium neodecanoate solution in xylene.

Table 3. Surface Area of the Reactant Powders.

Reactant	Method of preparation	Surface area (m^2/g)	Calculated spherical particle size (A^o)
$BaCO_3$	MOD	12.6	537
$BaCO_3$	Commercial (Amin et al.)	2.41	2809
TiO_2	MOD	132	59
TiO_2	Commercial (Amin et al.)	9.63	811
PbO	MOD (from Pb-acetate)	0.49	6480
PbO	MOD (from Pb-neodecanoate)	1.44	2200

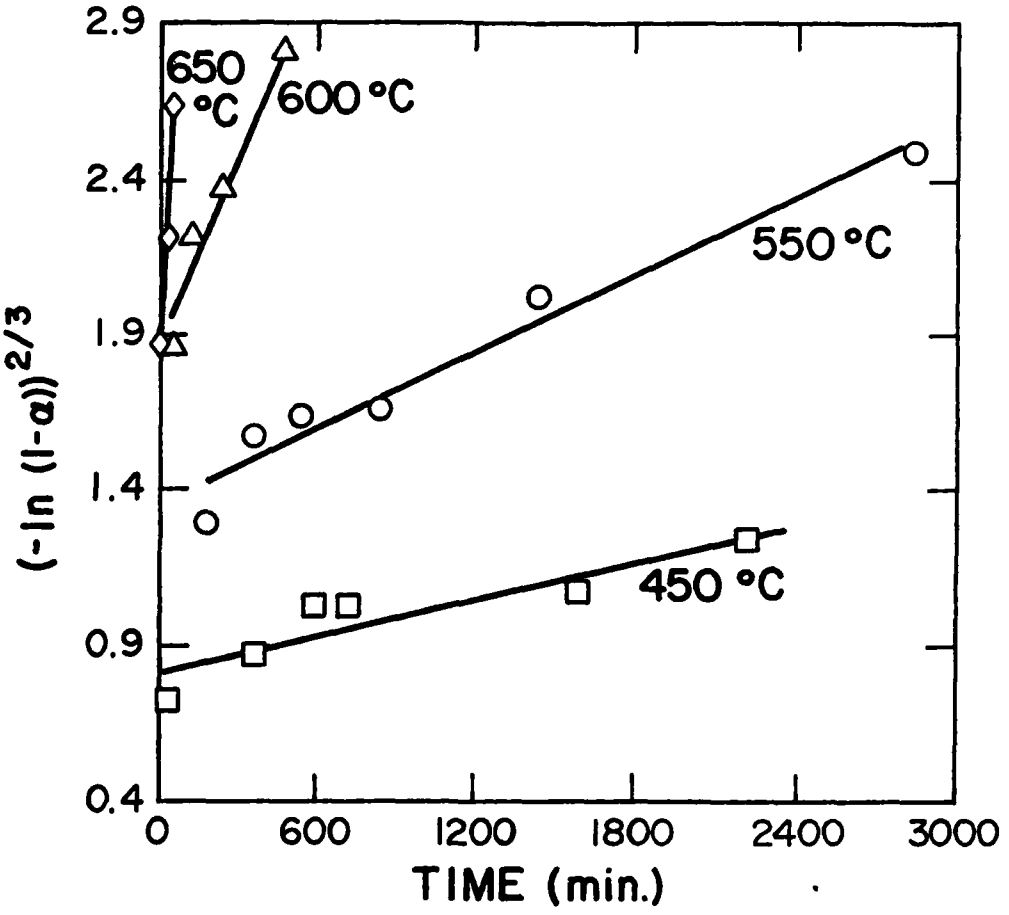

Figure 8. $(-\ln (1-\alpha))^{2/3}$ versus t plot for $PbTiO_3$ formation from lead acetate and titanium dimethoxy dineodecanoate.

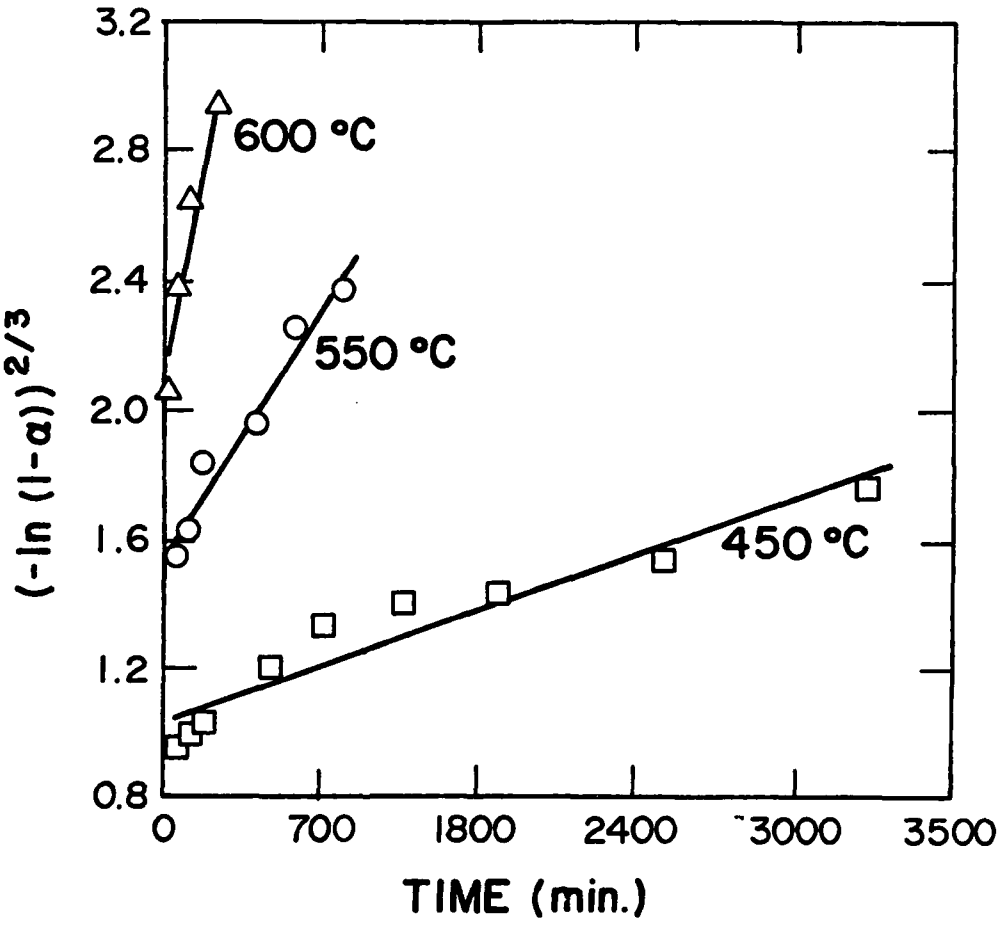

Figure 9. $(-\ln (1-\alpha))^{2/3}$ versus t plot for $PbTiO_3$ formation from lead neodecanoate and titanium dimethoxy dineodecanoate.

Table 4. Reaction Rate Constants for $PbTiO_3$ Formation.

Precursor	Temp (^oC)	K(sec^{-1})
	450	4.08×10^{-6}
Pb-neodecanoate	550	1.8033×10^{-5}
	600	6.485×10^{-5}
	450	3.4243×10^{-6}
Pb-acetate	550	6.849×10^{-6}
	600	3.4387×10^{-5}
	650	2.6843×10^{-4}

gives the reaction rate constant (k) of Eq. (1) obtained from these plots. In both cases the reactions are diffusion controlled. However, when lead-acetate was used as a precursor, the reaction preceded with zero nucleation rate, whereas, when lead neodecanoate was used as a precursor the reaction proceeded with a constant nucleation rate. The lead titanate kinetics data did not fit well to the Carter model.

Figure 10 is a plot of ln(k) versus (1/T) for $PbTiO_3$ formation from lead acetate and titanium dimethoxy dineodecanoate. The activation energy for $PbTiO_3$ formation using lead acetate as a precursor was 113 ± 18 kJ/mole, and similar studies using lead neodecanoate as a precursor yielded an activation energy of 93 ± 37kJ/mole.

Table 5 summarizes the cation diffusion data for the reactants involved in the present investigation. The Carter model [12] was developed for the oxidation of metals, where spherical metal particles are completely surrounded by gas. Since TiO_2 has a very fine grain size, the Carter model fits very well in this situation. The reported value for the activation energy for self diffusion of Ti in TiO_2 is 239 ± 20 kJ/mole [13-17]. similar values (232 kJ/mole and 240 kJ/mole) were obtained from the present studies using the Carter model. However, the activation energy values available in the literature for the rutile. Also, it is possible that the activation energy obtained in the present experiment correspond to self diffusion of Ti in $BaTiO_3$.

From Table 5 it is apparent that the self diffusion coefficients of Pb in PbO and Ti in TiO_2 do not differ nearly as much as do the self diffusion coefficients of Ba in BaO and Ti in TiO_2. Thus, the situa-

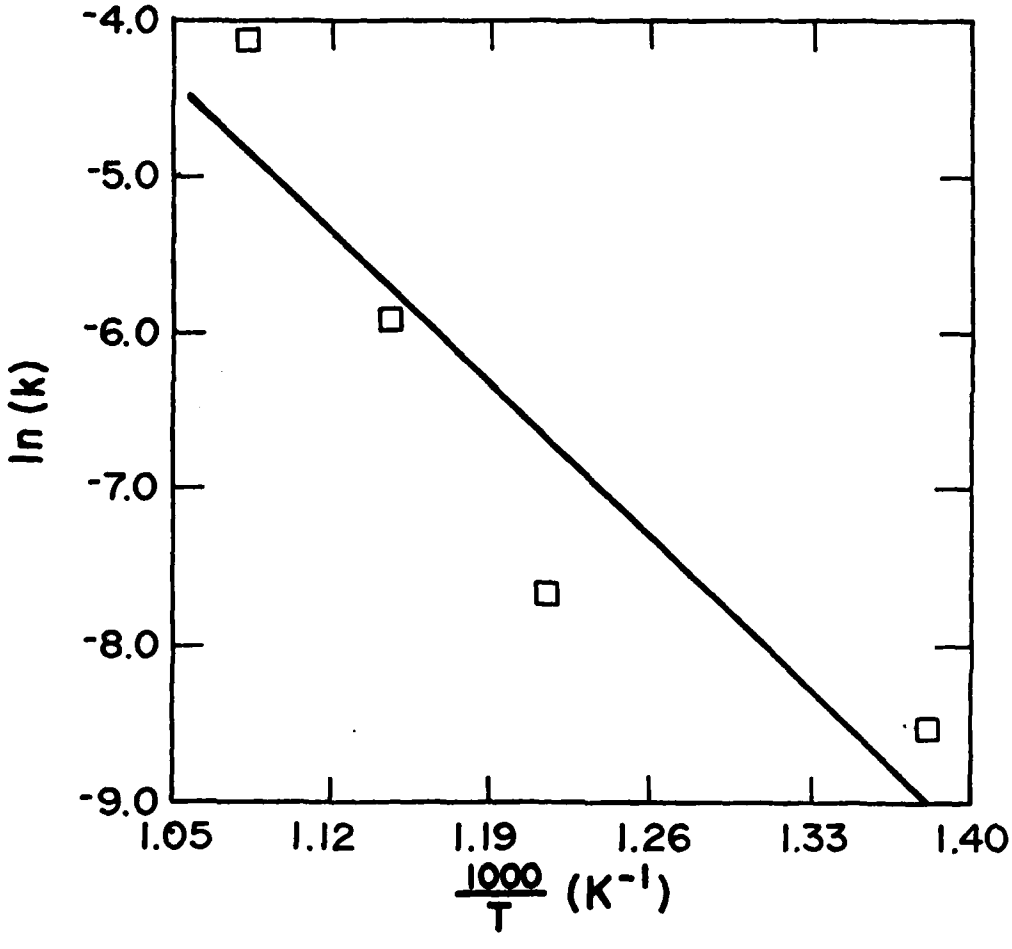

Figure 10. ln(k) versus (1/T) plot for $PbTiO_3$ formation from lead acetate and titanium dimethoxy dineodecanoate.

Table 5. Diffusion Data for Cations in the Reactants.

Reactant/Temp. (^{o}C)	D Diffusion coefficient (m^2/sec) 450	500	550	Q kJ/mole	D_o m^2/sec.
TiO_2 [14]	1.51×10^{-24}	2.42×10^{-23}	4.04×10^{-22}	257*	6.4×10^{-6}*
PbO [13]	1.12×10^{-19}	2.18×10^{-18}	2.97×10^{-17}	276	10
BaO [13]	3.28×10^{-52}	2.91×10^{-47}	6.45×10^{-43}	1059*	10^{25}*

*Values are for higher temperature range and for single crystals.

tions in $BaTiO_3$ formation and $PbTiO_3$ formation are different. Activation energies deduced from the experiments ($\simeq$ 100 kJ/mole) are considerably less then the activation energies for self diffusion of lead or titanium indicated in Table 5.

2.4 Summary

Formation of compounds from metallo-organic precursors takes place at a much lower temperature and at a much faster rate as compared to that from powder precursors. This is the result of the extremely fine grain size of the decomposed product and the mixing on the atomic level.

Barium titanate formation from metallo-organic precursors was found to be a diffusion controlled reaction. The activation energy for diffusion obtained from the kinetic model was similar to that of the activation energy for self diffusion of Ti in TiO_2. The lead titanate formation reaction was also found to be diffusion controlled, but the activation energy was found to be low and did not correspond to any known activation energy for diffusion.

3. DEFECT STRUCTURE AND ELECTRICAL PROPERTIES OF Nd_2O_3 MODIFIED $BaTiO_3$

3.1 General

Numerous studies on the effect of various modifiers on the dielectric and structural properties of barium titanate have been reported.

Modifying ions having the same charge as one of the host cations can replace that cation without producing any additional point defects. The solid solubility limit in such substitution is determined by the ionic sizes and electronic structures of the cations involved. However, when a cation with different oxidation state than that of the host cation replaces the host cation, a defect structure may be produced for charge compensation. Rare earth ions fall under this catagory.

Barium titanate doped lightly with trivalent rare earth ions acts as a semiconductor, and ceramic samples show an analogous dependence of resistivity on temperature. A number of papers have been published concerning the electrical properties of rare earth doped barium titanate [18-23]. Electrical properties of rare earth doped $BaTiO_3$ are very sensitive to the doping level. Various studies [21, 23, 24] indicate that $BaTiO_3$ acts as a semiconductor up to about 0.3 mole % of additions of rare earth ions, and above that as an insulator. Different explanations have been given for this behavior. R. Wernicke [24] explained this effect based on the grain size and kinetics of diffusion. J. B. MacChesney et al. [23] attributed the effect to the presence of different defect structures in the different composition regimes. They assumed that up to 0.25 mole% addition of rare earths to $BaTiO_3$, charge compensation takes place by the conversion Ti^{4+} to Ti^{3+}, and above that by formation of barium vacancies as shown in Eq. (5) and Eq. (6).

$$BaTiO_3 + xLa_2O_3 \cdot 2TiO_2 \rightarrow Ba_{Ba} + 2xLa^{\cdot}_{Ba} + Ti_{Ti} + 2xTi'_{Ti} + (3+6X)O_O + \frac{x}{2}O_2 \quad (5)$$

$$BaTiO_3 + xLa_2O_3 \cdot 3TiO_2 \rightarrow Ba_{Ba} + 2xLa_{Ba} + xV_{Ba}^{\cdot\cdot} + (1+3x)Ti_{Ti} + (3+9x)O_O \quad (6)$$

Recently, Chan and Smyth [25] postulated reactions represented by Eq. (7) and Eq. (8) for lower and higher doping levels respectively.

$$2La_2O_3 + 4TiO_2 \rightarrow 4La^{\bullet}_{Ba} + 4Ti_{Ti} + 12O_o + O_2 + 4e' \quad (7)$$

$$2La_2O_3 + 6TiO_2 \rightarrow 4La^{\bullet}_{Ba} + 6Ti_{Ti} + 18O_o + 2V''_{Ba} \quad (8)$$

J. B. McChesney et al.[23] also reported that longer firing and the absence of a grain boundary phase gave higher resistivity. This result contradicts the theory suggested by R. Wernicke [24], according to which large grained material should have lower resistivity.

Since lightly doped material had excellent semiconducting properties and a temperature dependence of resistivity which was of interest for thermistor applications, the early studies [18-23] were restricted to very low levels of doping. Also, the defect structures were mainly assumed. Saburi [21], who studied the effect of very low levels of additions of Pr, Sm, Bi, Ce, Ta, Nb, Nd, Sb, La and Ta on electrical properties of $BaTiO_3$, proposed that the lanthanides occupy the barium site and charge compensation takes place by a change in the oxidation state of the titanium ion from +4 to +3. A similar defect structure was also postulated by Tekster et al [22].

Mazdiyasni and Brown [26] reported the absence of any second phase up to 0.2 mole% additions of La_2O_3 and Nd_2O_3 to $BaTiO_3$. Vojnovich and McGee [27] did not notice any second phase up to 1 mole% Gd doping. However they felt, based on the smaller grain size of doped sample compared to the undoped sample, that a second phase might be present at the grain

boundaries. At low doping levels, detection of a second phase by x-rays is extremely difficult. Thus, x-ray diffraction results at low doping levels often do not lead to any conclusion. T. Ikeda and A. Watanabe [28] used ESR (Electron Spin Resonance) to study the defect structure of Gd-doped $BaTiO_3$. Their observations suggested the presence of Gd^{3+} ion on both barium and titanium sites.

A few studies have been reported about the characterization of the defect structure of La_2O_3 doped $PbTiO_3$[29-31], $SrTiO_3$ [32] and $BaTiO_3$ [33] at higher doping levels. The present study was designed to gain some understanding about the defect structure of Nd_2O_3-$BaTiO_3$, and to study the effect of moderate levels of doping of Nd_2O_3 on the dielectric properties of $BaTiO_3$.

3.2 Approach

Barium titanate has the perovskite structure with high packing density, which makes interstitial atoms unlikely. G. V. Lewis and C. R. A. Catlow's [34] defect energy calculations also indicate that the formation of interstitials is unlikely. Thus, in the present study only substitutional solid solutions were considered.

Since the neodymium ion has a different valance than that of the barium or titanium ion, substitution by neodymium for one of these produces a charge imbalance and charge compensation requires that electrons, electron holes or vacancies be produced. The dielectric loss values observed in the present investigation were too low to consider electrons or electron holes as the charge compensating species. Thus,

charge compensation by various types of vacancies were the only possibilities considered.

Table 6 lists the various defect structures considered and their unit cell formulae. Formulations A and E were prepared based on the assumption that the substitution occurs at the barium site and charge compensation takes place by formation of $V_{Ba}^{''}$ and $V_{Ti}^{''''}$ respectively. Formulation D was prepared based on the assumption that substitution occurs the titanium site and charge compensation takes place by creation of oxygen vacancies. Formulation C assumes self compensation. Formulation B was considered to investigate the possibility of a $Nd_2O_3.2TiO_2$-$BaTiO_3$ join.

3.3 Experimental

3.3.1 Materials

As discussed in Section 2, barium titanate was formed at very low temperatures using the metallo-organic compounds barium neodecanoate and titanium dimethoxy dineodecanoate, as precursors. Xylene solutions of these compounds were mixed in equimolar proportion to obtain a formulation which on thermal decomposition gave $BaTiO_3$. Since the formulation prepared using solutions of metallo-organic compounds is a mixture of true solutions, mixing of barium, titanium and other compounds if added is expected to be on a molecular level. This fact is expected to give homogeneity on the molecular level, which will produce the thermodynamically stable phase or phases much more quickly than if powders of the constituents are mixed and fired.

Table 6. List of Defect Structures Considered.

Mix	Charge compensation	Mix $BaTiO_3$ plus
A	$[Nd_{Ba}^{\cdot}] = 2[V_{Ba}^{''}]$	$Nd_2O_3 \cdot 3TiO_2$
B	$[Nd_{Ba}^{\cdot}] = 2[V_{Ba}^{''}] + 4[V_{Ti}^{''''}]$ and $[V_{Ba}^{''}] = [V_{Ti}^{''''}]$	$Nd_2O_3 \cdot 2TiO_2$
C	$[Nd_{Ba}^{\cdot}] = [Nd_{Ti}^{'}]$	Nd_2O_3
D	$[Nd_{Ti}^{'}] = 2[V_o^{\cdot\cdot}]$	$Nd_2O_3 \cdot 2BaO$
E	$[Nd_{Ba}^{\cdot}] = 4[V_{Ti}^{''''}]$	$Nd_2O_3 \cdot \frac{3}{2} TiO_2$

	Unit Cell Formula
A	$[(Ba_{Ba})_{1-3x} (Nd_{Ba}^{\cdot})_{2x} (V_{Ba}^{''})_x] TiO_3$
B	$[(Ba_{Ba})_{1-7x/3} (Nd_{Ba}^{\cdot})_{2x} (V_{Ba}^{''})_{x/3}] [(Ti_{Ti})_{1-x/3} (V_{Ti}^{''''})_{x/3}] O_3$
C	$[(Ba_{Ba})_{1-x} (Nd_{Ba}^{\cdot})_x] [(Ti_{Ti})_{1-x} (Nd_{Ba}^{'})_x] O_3$
D	$Ba[(Ti_{Ti})_{1-2x} (Nd_{Ti}^{'})_{2x}] [(O_o)_{3-x} (V_o^{\cdot\cdot})x]$
E	$[(Ba_{Ba})_{1-2x} (Nd_{Ba}^{\cdot})_{2x}] [(Ti_{Ti})_{1-x/2} (V_{Ti}^{''''})_{x/2}] O_3$

Barium neodecanoate and titanium dimethoxy dineodecanoate were prepared following the procedures described in Section 2. Neodymium neodecanoate was prepared by reacting the ammonium soap of neodecanoic acid, obtained by reacting ammonium hydroxide with neodecanoic acid, with an aqueous solution of neodymium chloride. The neodymium neodecanoate was separated from the aqueous phase and dissolved in xylene.

The thermal decomposition behavior of the compounds was studied using thermogravimetric analysis. Figure 11 shows the thermogram of neodymium neodecanoate. The rapid weight loss below $100^{o}C$ is due to evaporation of the xylene solvent, and the remaining weight loss represents the decomposition of neodymium neodecanoate. The corresponding thermograms for barium neodecanoate and titanium dimethoxy dineodecanoate were shown in Figs. 1 and 2. Table 7 lists the decomposition temperatures at a heating rate of $10^{o}C$/min. for all three compounds. The decomposition products were characterized using x-ray diffraction.

3.3.2 Sample Preparation

The metallo-organic compounds in xylene required for a particular formulation were weighed to 0.005 g, and mixed thoroughly by manual stirring for a few minutes. The solution was then heated from $200^{o}C$ to $\sim 450^{o}C$ at the heating rate of $\sim 10^{o}C$/min. The residue was further heated to about $650^{o}C$ for complete decomposition. The kinetic studies in Section 2 showed that an equimolar mixture of the Ba and Ti compounds formed $BaTiO_3$ at $660^{o}C$ at a heating rate of $5^{o}C$/min. This solid mass was pulverized manually and approximately 0.15 g of the powder was pressed at about 80,000 psi. to obtain a disk shaped pellet (dia ~6 mm,

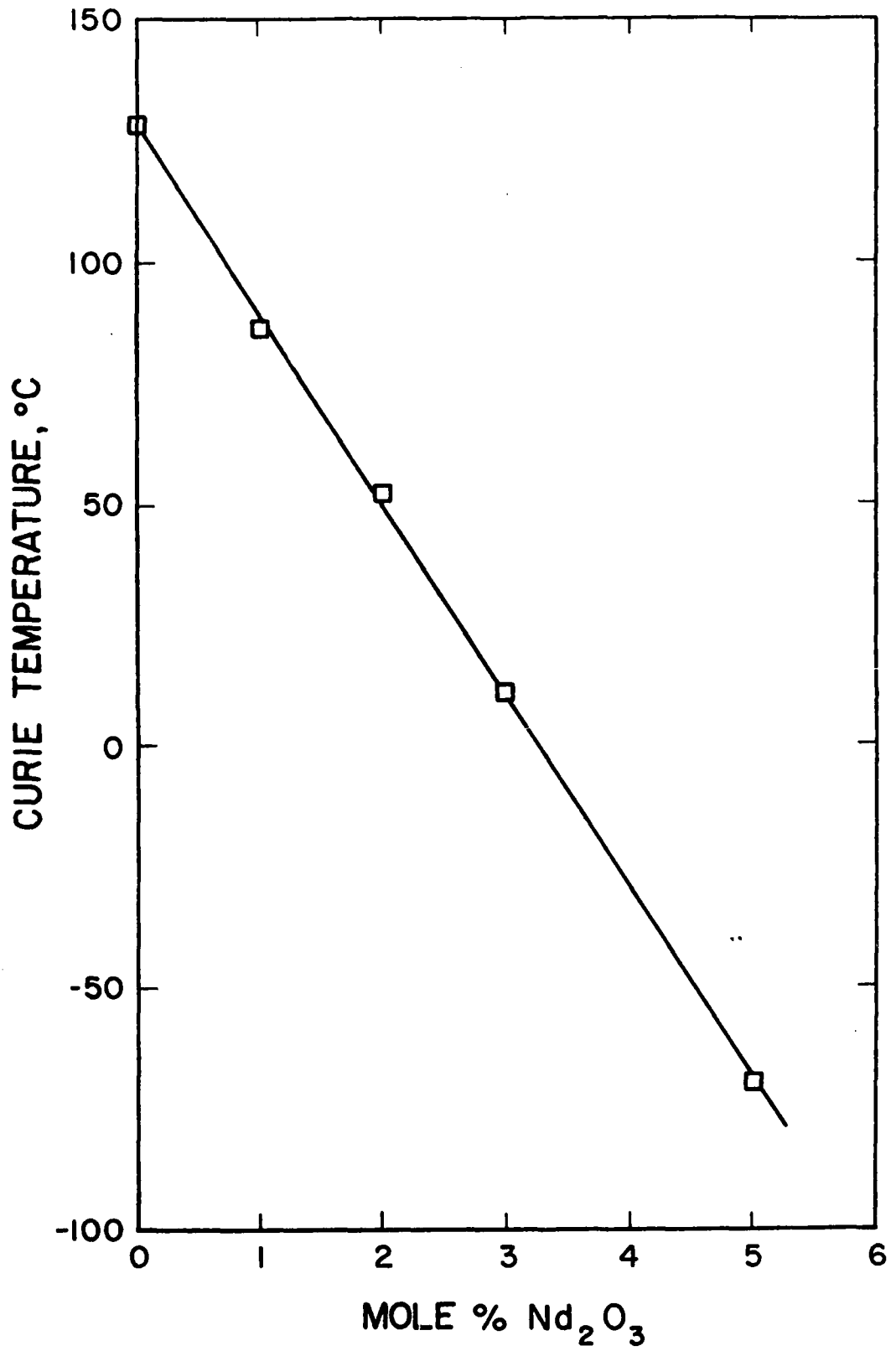

Figure 15. Variation of Curie temperature of formulation E with mole % Nd_2O_3.

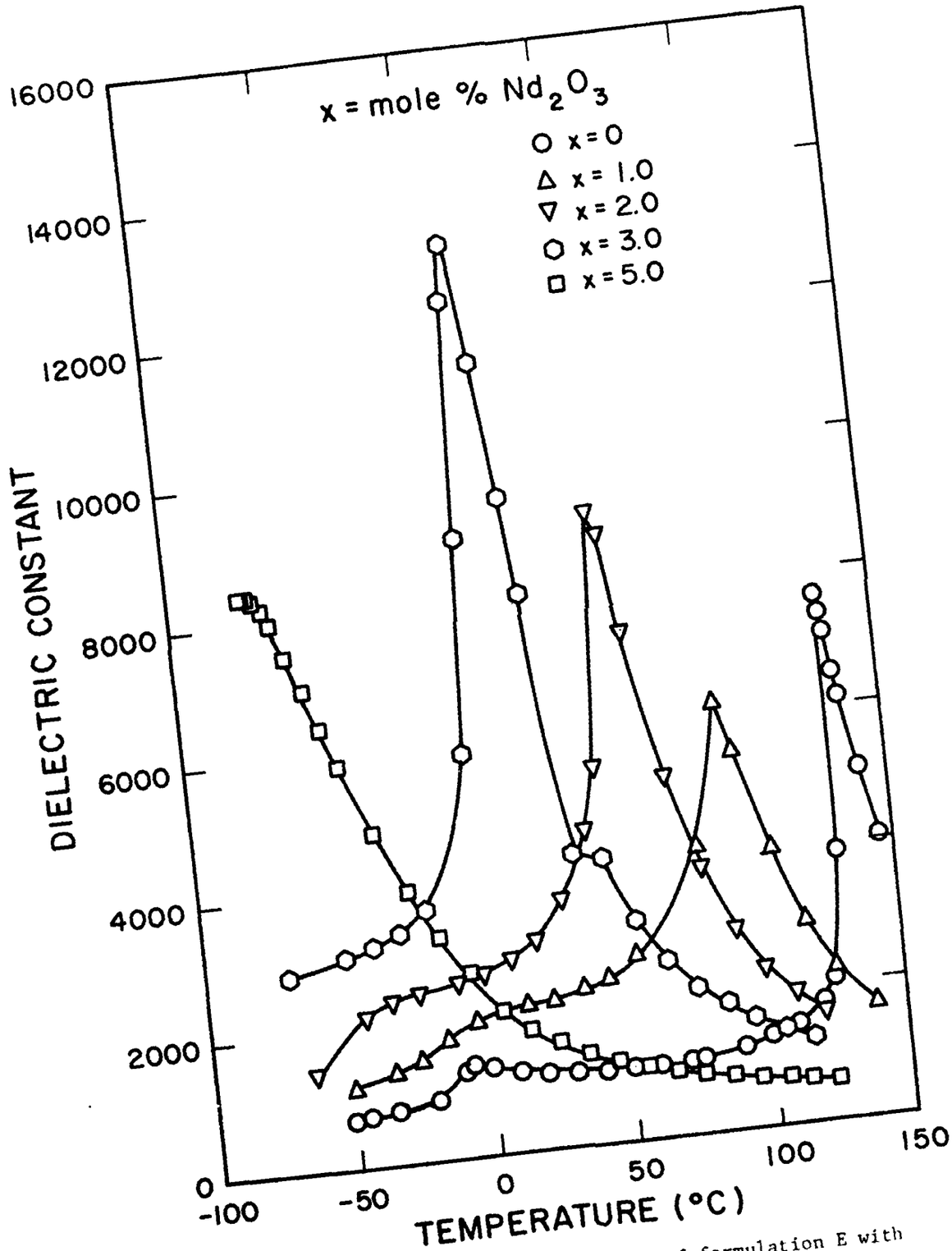

Figure 14. Variation of dielectric constant of formulation E with temperature.

$$BaO + (1-2x)TiO_2 + xNd_2O_3 \rightarrow$$

$$\frac{2(1-2x)}{2-x}\left|(Ba_{Ba}^{x})_{1-2x}(\dot{Nd}_{Ba})_{2x}\right|\left|(V_{Ti}^{''''})_{x/2}(Ti_{Ti}^{x})_{1-\frac{x}{2}}\right|O_3$$

$$+ \frac{x(7-8x)}{(2-x)}BaO + (\frac{3x^2}{2-x})Nd_2O_3 \qquad (12)$$

From Eq. (9) and Eq. (10), the ratio of rejected Nd_2O_3 and TiO_2 is identically equal to $\frac{2x}{3(1-x)}$, and the x-ray diffraction pattern of formulations A and B indicated the presence of the same second phase. Eq. (11) and Eq. (12) suggest that the second phase in formulations C and D should be BaO rich. The x-ray diffraction pattern of formulation D confirmed the presence of orthorhombic Ba_2TiO_4. The x-ray diffraction pattern of formulation C indicated the presence of an unknown phase, although a few of the peaks corresponded to Ba_2TiO_4. This was expected because according to Eqs. (11) and (12), the rejected $BaO:Nd_2O_3$ ratio is slightly higher for formulation C than for formulation D.

3.4.2 Dielectric Properties

Figure 14 shows the variation of dielectric constant with temperature for various compositions of formulation E. Addition of Nd_2O_3 decreases the Curie temperature of barium titanate drastically as shown in Fig. 15; Nd_2O_3 . 3/2 TiO_2 is a more effective Curie point depressor for $BaTiO_3$ than any previously reported compound. At 5 mole % Nd_2O_3 addition, samples made from the other four formulations did not show as low of a Curie temperature as did formulation E, which is the expected

i) Formulation A-

$$(1-3x)BaO + TiO_2 + xNd_2O_3 \rightarrow$$

$$\frac{3x-1}{2x-1}\left|(Ba^{x}_{Ba})_{1-2x}(\dot{Nd}_{Ba})_{2x}\right|\left|(V_{Ti}^{''''})_{x/2}(Ti^{x}_{Ti})_{1-\frac{x}{2}}\right|O_3$$

$$+ \frac{3x}{2}(\frac{x-1}{2x-1})TiO_2 + (\frac{x^2}{1-2x})Nd_2O_3 \qquad (9)$$

ii) Formulation B

$$(1-\frac{7x}{3})BaO + (1-\frac{x}{3})TiO_2 + xNd_2O_3 \rightarrow$$

$$\frac{1}{3}(\frac{7x-3}{2x-1})\left|(Ba^{x}_{Ba})_{1-2x}(\dot{Nd}_{Ba})_{2x}\right|\left|(V_{Ti}^{''''})_{x/2}(Ti^{x}_{Ti})_{1-\frac{x}{2}}\right|O_3$$

$$+ (\frac{x^2}{3(1-2x)})Nd_2O_3 + \frac{3x}{2}(\frac{x-1}{3(2x-1)})TiO_2 \qquad (10)$$

iii) Formulation C

$$(1-x)BaO + (1-x)TiO_2 + xNd_2O_3 \rightarrow$$

$$\frac{2x-2}{x-2}\left|(Ba^{x}_{Ba})_{1-2x}(\dot{Nd}_{Ba})_{2x}\right|\left|(V_{Ti}^{''''})_{x/2}(Ti^{x}_{Ti})_{1-\frac{x}{2}}\right|O_3$$

$$+ \frac{3x(1-x)}{(2-x)}BaO + (\frac{x^2}{2-x})Nd_2O_3 \qquad (11)$$

iv) Formulation D

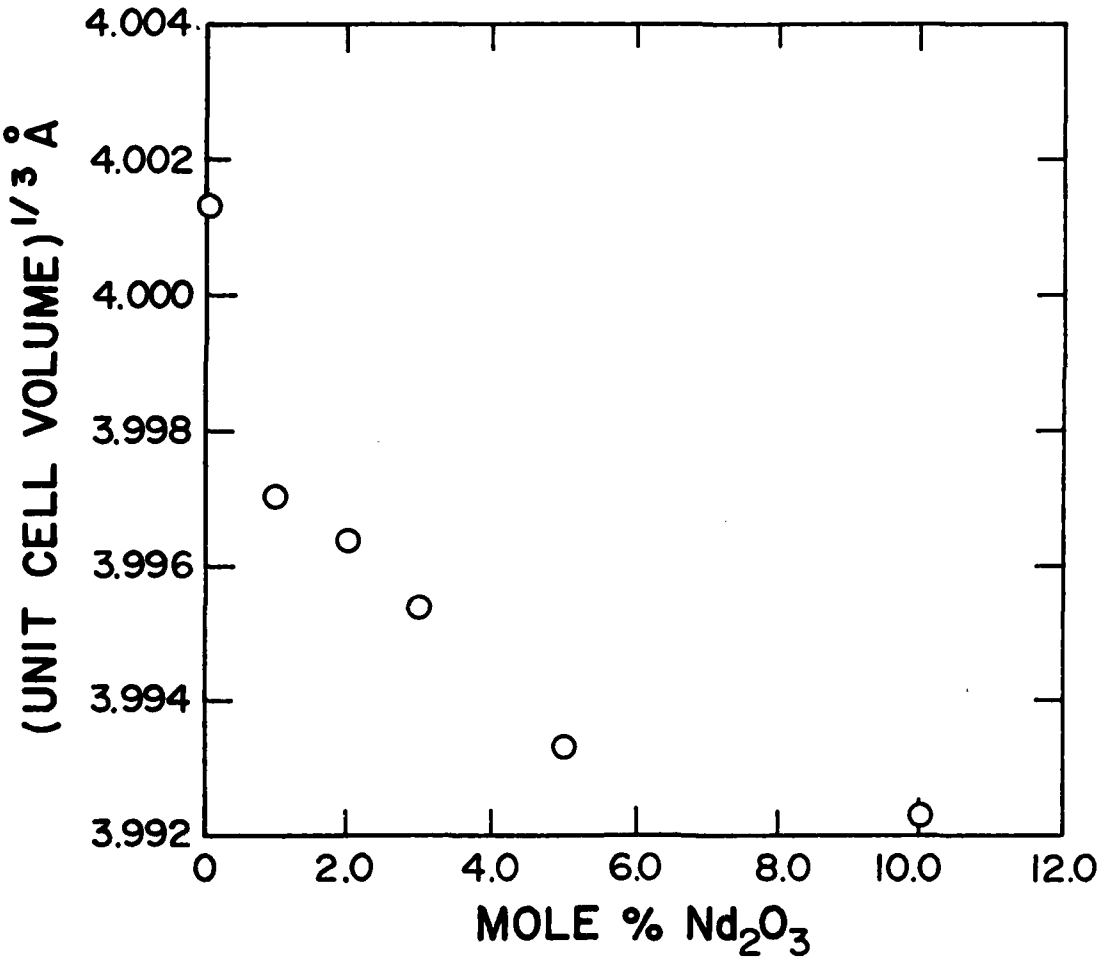

Figure 13. Variation of (unit cell volume)$^{1/3}$ of formulation E with mole % Nd_2O_3.

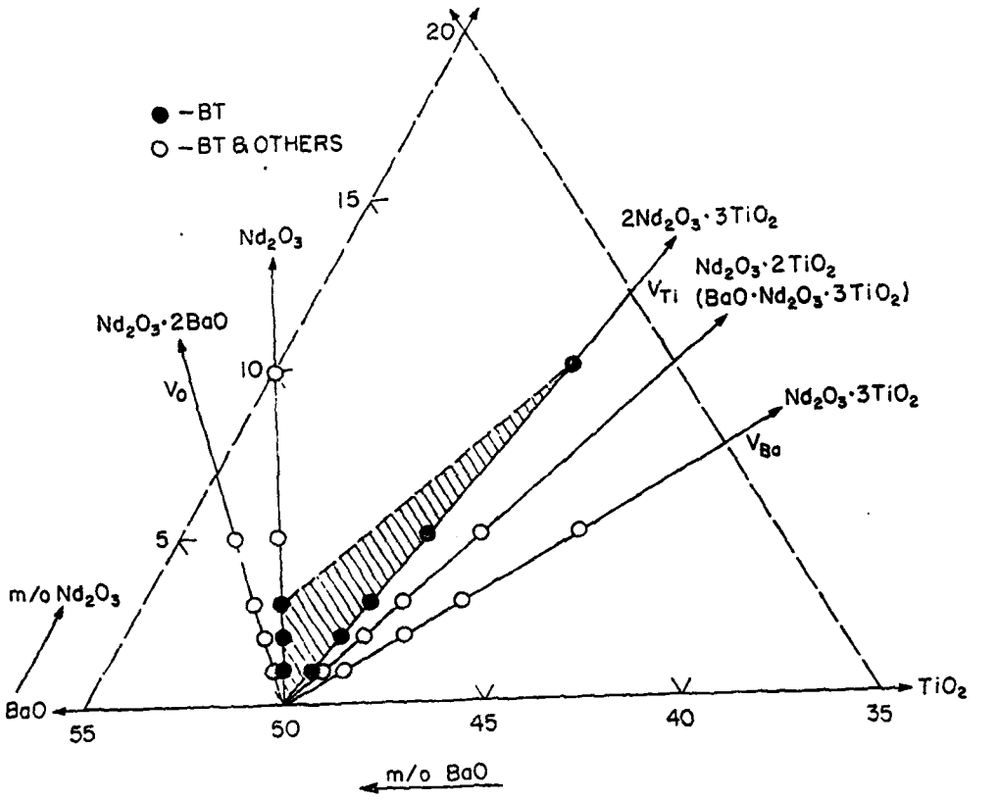

Figure 12. A segment of the BaO - Nd_2O_3 - TiO_2 phase diagram.

Table 10. 'd' Spacings and Relative Intensities for Unknown Phases.

α phase/phases		β phase/phases	
d	Relative intensity	d	Relative intensity
3.19	67	3.28	28
2.09	47	3.12	46
2.98	67	3.07	23
2.78	67	3.02	81
2.72	67	2.98	100
2.63	67	2.68	12
2.11	47	2.21	16
1.93	47	2.12	35
1.74	80	1.92	12
1.7	40	1.9	12
1.62	40	1.85	12
1.6	100	1.82	33
1.58	47	1.81	33
		1.73	23

Table 9. Compounds not Detected in α and β.

BaO	Ba_2TiO_4	Nd_2TiO_5
TiO_2	$BaTi_2O_5$	$Nd_2Ti_2O_7$
Nd_2O_3	$Ba_2Ti_5O_{12}$	$Nd_2Ti_4O_{11}$
	$Ba_6Ti_{17}O_{40}$	$Nd_4Ti_9O_{24}$
	$BaTi_3O_7$	
	$Ba_4Ti_{13}O_{30}$	
	$BaTi_4O_9$	$BaNd_2Ti_3O_{10}$
	$Ba_2Ti_9O_{20}$	$BaNd_2Ti_5O_{14}$
	$BaTi_5O_{11}$	

presence of a second phase or phases (β). The α and β phases were not any of the phases listed in Table 9, although a few of the peaks in the β phase matched with those of Ba_2TiO_4. The d spacings and approximate intensities for the α and β phases are listed in Table 10. Formulation D showed a second phase or phases (γ) at all Nd_2O_3 levels. Most of the diffraction peaks in γ correspond to the orthorhombic form of Ba_2TiO_4, but a few extra peaks were observed. No second phase was observed for formulation E at any level of Nd_2O_3 addition studied. Figure 12 summarizes the various compositions studied on a portion of the BaO - TiO_2 - Nd_2O_3 composition triangle. The shaded portion corresponds to the single phase region suggested by this study.

Lattice parameters of samples made from formulation E were determined and the unit cell volumes calculated from these results are displayed in Fig. 13. The unit cell volume decreased continuously as Nd_2O_3 was added to $BaTiO_3$, which indicates that the smaller neodymium ion replaces the larger barium ion. This is consistent with the defect structure assumed for formulation E. Formulations E containing 1 and 2 mole% Nd_2O_3 were found to be tetragonal while the rest were cubic. The unit cell volume of solid solutions does not extrapolate to $BaTiO_3$. Similar observations were made by G. H. Jonker et al. [33] in the $BaTiO_3$-La_2O_3 system.

The phase analysis results suggest that the defect structure assumed for formulation E is the correct one. If the Nd ion goes into the barium site and charge compensation takes place by creation of titanium vacancies, then the following reactions are expected for the various formulations:

Table 8. Summary of X-Ray Diffraction Phase Analysis.

Crystalline Phases Detected (BT = $BaTiO_3$, $\gamma = Ba_2TiO_4$)

	Mole percent Nd_2O_3				
Mix	1	2	3	5	10
A	BT + α	BT + α	BT + α	BT + α	-
B	BT + α	BT + α	BT + α	BT + α	BT + α
C	BT	BT	BT	BT + β	BT + β
D	BT + γ	BT + γ	BT + γ	BT + γ	BT + γ
E	BT	BT	BT	BT	BT

α and β could not be identified

nature of the latent heat peak. Thus, a specimen of the same weight as that of the sample but with a different Nd_2O_3 doping level, hence a different Curie temperature, was used as a reference.

For the structural analysis, an automated x-ray diffractometer* was used. The phase analysis was done using 2° (2θ)/min detector scan speed and cobalt and copper radiation. From the phase analysis data, the high angle reflections of the respective phases were chosen for the lattice parameter determination. Determination of the lattice constants of the phase was done by using a lattice constant refinement program [26], which refines lattice constants for any symmetry by the least square method.

3.4 Results and Discussion

3.4.1 Structural Studies

Very little work has been done on the $BaO - TiO_2 - Nd_2O_3$ system, and most of the reported studies considered titanium rich compositions [37-39]. Table 8 summarizes the results of the x-ray phase analyses. Diffraction patterns of formulation A containing 1, 2, 3 and 5 mole% $Nd_2O_3 \cdot 3TiO_2$ and formulation B containing 1, 2, 3, 5 and 10 mole% $Nd_2O_3 \cdot 2TiO_2$ indicated the presence of a similar second phase or phases (α) which could not be identified. No second phase was observed for formulation C at 3 mole% Nd_2O_3 or less, but higher Nd_2O_3 additions showed the

Dupont #910, Dupont Inc., Wilmington DE.

* Kristalloflex 4, Siemens Inc. Germany.

thickness ~1.25 mm). The pellet was placed on a bed of powder of the same composition in a platinum crucible and fired at 1340°C-1370°C for 2 hours. The powder was used for subsequent structural studies. The sintered pellets were painted with a Pd-Ag thick film conductor composition[+++], dried at 200°C and fired at 850°C for about 15 minutes. Thin copper wires were soldered to both sides of the sample. To avoid the effects of moisture, the samples were coated with a protective spray[**].

3.3.3 Measurement of Properties

The dielectric properties of the samples were measured as a function of temperature. An environmental chamber[+] was used to vary the temperature of the sample atmosphere from -80°C to +160°C. The temperature of the specimen was checked with the help of alumel-chromel microthermocouple kept very close to the specimen.

The dielectric constant and the dissipation factor of the specimens were measured using a digital LCR meter[#$]. All the dielectric properties were measured at 1kHz test frequency and using zero D. C. bias. Spontaneous polarization measurements were carried out using the hysteresis loop bridge circuit suggested by Diamant et al. [35]

Specific heat measurements were carried out using a differential scanning calorimeter[#]. The basic interest of this study was to find the

+++ No. 6120, DuPont Inc., Niagara Falls, N. Y.

** Crystal Clear,No. 1302, Borden Inc., Columbus,

+ Model SK 2101,Associated Testing Laboratories Inc., Wayne, NJ.

#$ No. 4262A Hewlett Packard Inc., Palo Alto, CA.

Table 7. Thermogravimetric Analysis Results.

Compound	Decomposition temp. (^{o}C)	Product
Barium neodecanoate	387	$BaCO_3$
Titanium dimethoxy dineodecanoate	325	TiO_2 (anatase)
Neodymium neodecanoate	375	Nd_2O_3

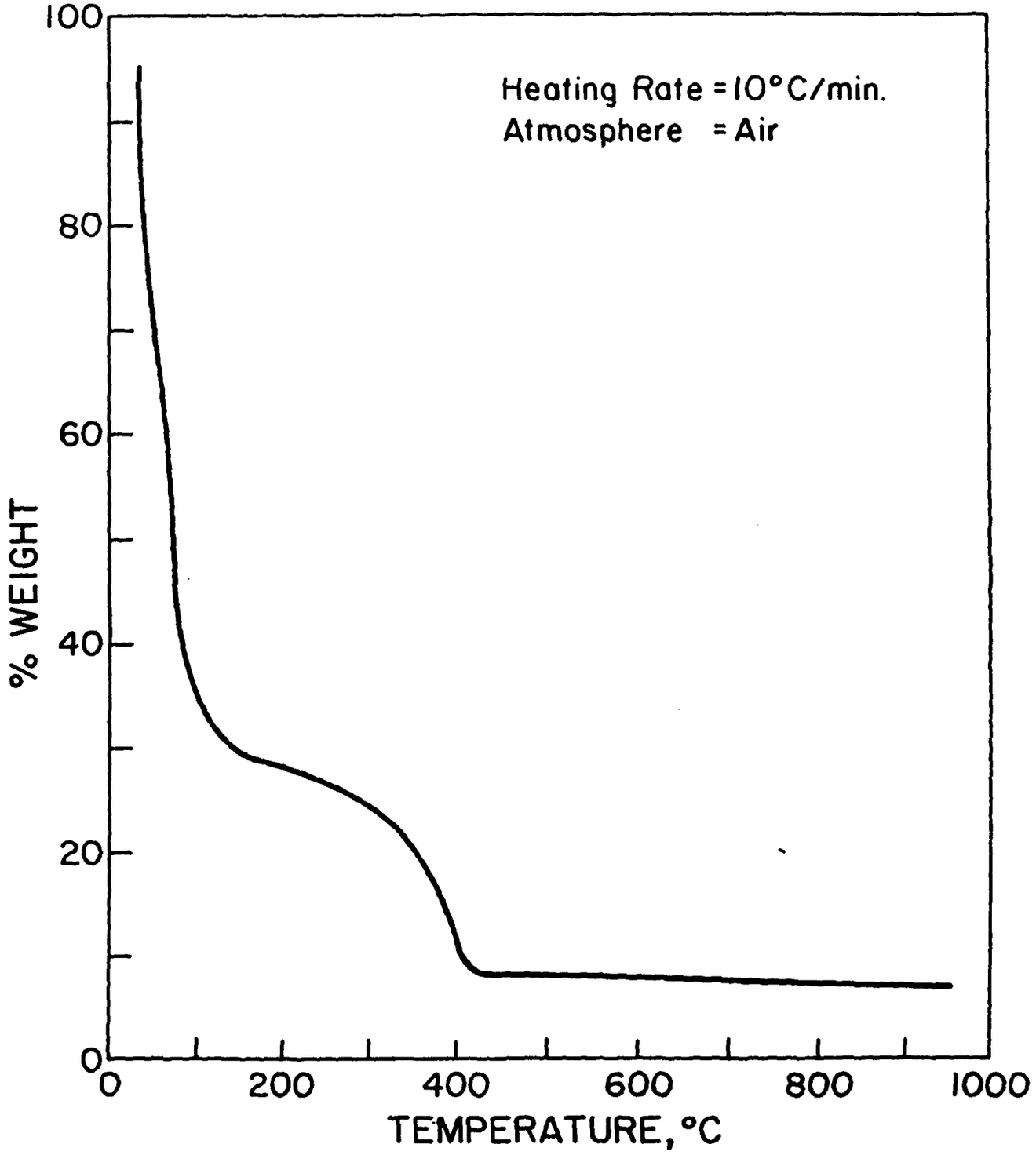

Figure 11. Thermogram of neodymium neodecanoate solution in xylene.

behavior for two phase mixtures. However, the Curie temperatures of 1, 2 and 3 mole % Nd_2O_3 samples of formulation C agreed quite well with the corresponding samples of formulation E. All of these samples had single phase x-ray diffraction patterns.

Figure 16 shows the variation of dissipation factor with temperature for various compositions of formulation E. The Curie temperature corresponds to the point of inflection of the dissipation factor vs. temperature curves of the doped samples. The dielectric loss versus temperature curve can be divided into two regions. Region I is below the Curie point where the higher losses are caused primarily by domain walls, and the low loss region just above the Curie temperature is region II. The dissipation factors in region I were typically about 0.03, and those in region II less than 0.001, indicating the absence of electrons or holes. The dissipation factor of the composition containing 1 mole % Nd_2O_3 showed an increasing trend as temperature was reduced below the Curie point. This could be due to the tetragonal-orthorhombic phase transition. Since this phase transition was not observed in the samples containing 3 or more mole% Nd_2O_3, their dissipation factors did not show the increasing trend after reaching some high dissipation factor value below the Curie point.

Figure 17 shows the variation of inverse susceptibility with temperature for various compositions of formulation E. The temperature θ at which the inverse susceptibility becomes zero was obtained by extrapolation. For undoped $BaTiO_3$, the difference $\theta - T_c$ was about $10^{o}C$, which is in agreement with a previous observation [40]. Temperature $\theta > T_c$ is a typical characteristic of a first order transformation. As the doping

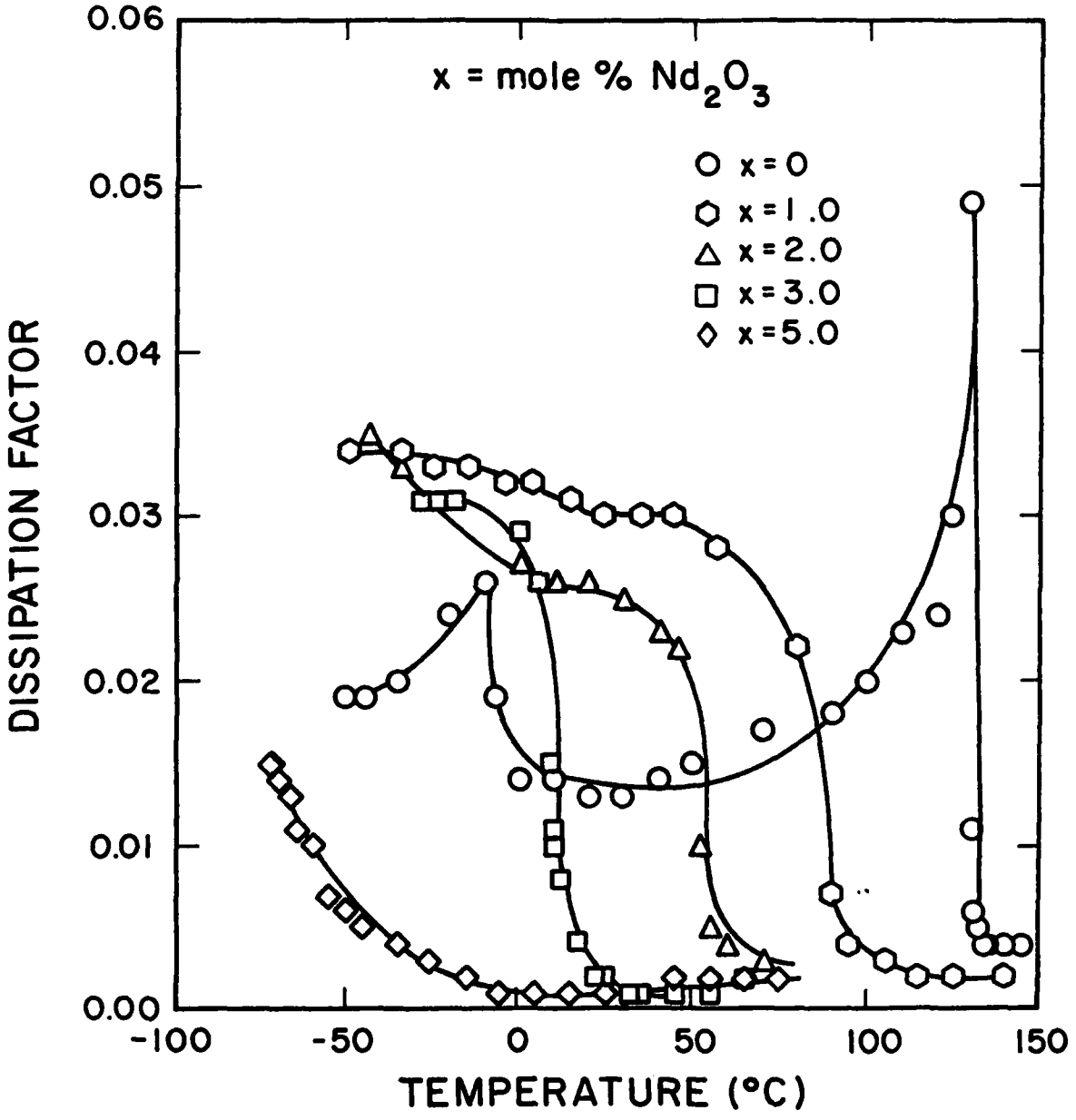

Figure 16. Variation of dissipation factor of formulation E with temperature.

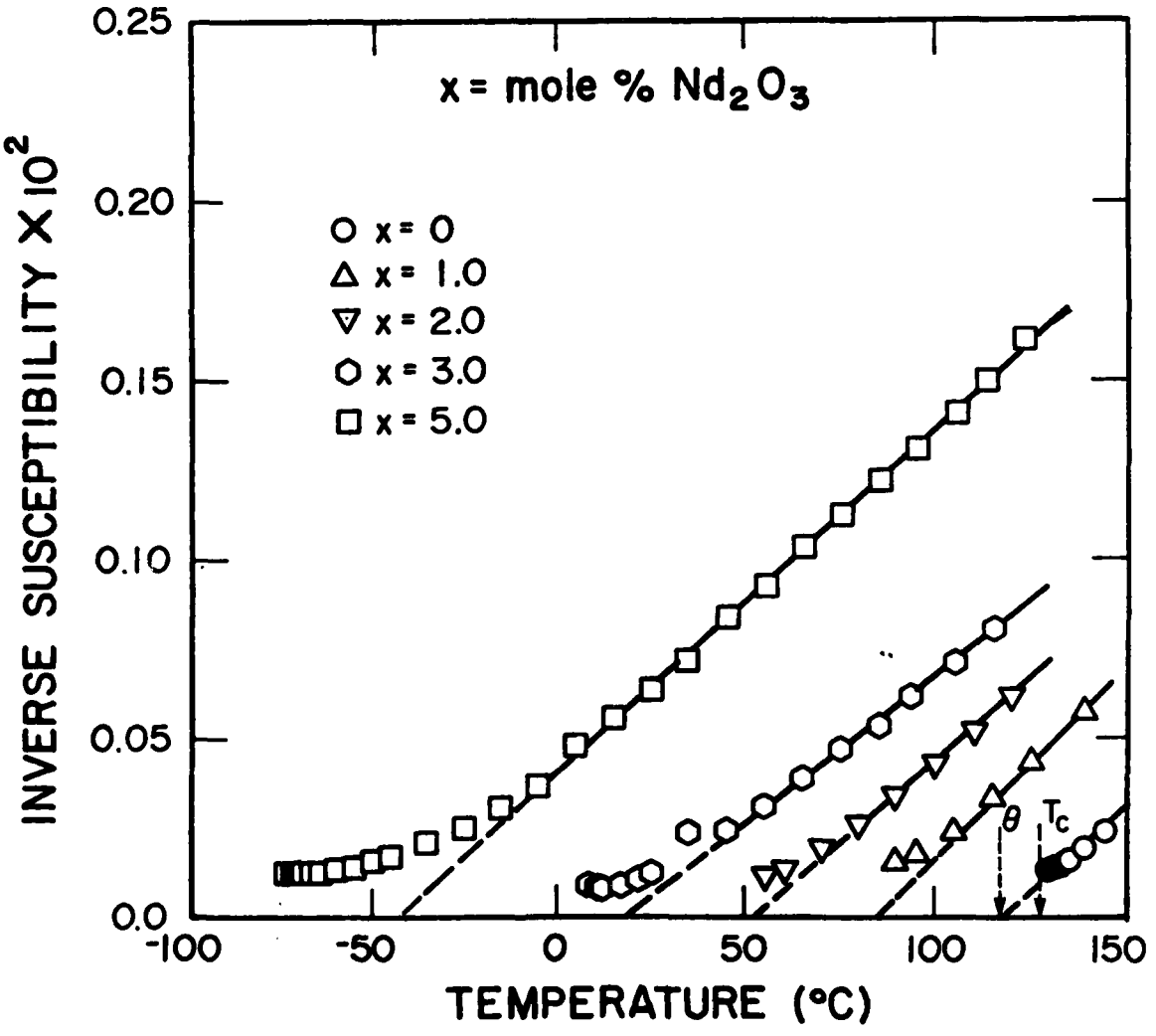

Figure 17. Variation of inverse susceptibility of formulation E with temperature.

level increased, the difference ($\theta - T_c$) decreased. At 2 mole% addition of Nd_2O_3, T_c was approximately equal to θ, and above 2 mole% addition T_c was greater than θ. This indicates that the ferroelectric phase transformation is becoming diffuse. This phenomenon was observed by G. Godefroy et al. [41] in Co-doped $BaTiO_3$ and by S. Kuroda and K. Kubota [42] in rare earth doped SBN. N. Setter and L. E. Cross [43] explained the diffuse phase transformation behavior of perovskite ferroelectrics on the basis of order-disorder of B-site cations. An ordered crystal shows a normal first order transformation behavior, whereas disorder contributes to local composition fluctuations and causes a diffuse phase transformation. A. P. Lavaynuk and A. S. Sigov [44] gave a quantitative explanation of this behavior based on the ordering of defects.

To confirm the nature of the phase transformations, spontaneous polarization and specific heat experiments were conducted. Figure 18 shows the variation of spontaneous polarization with temperature for three compositions of formulation E. The rate of increase of spontaneous polarization with temperature is slower for the formulations containing higher amounts of Nd_2O_3, which is consistent with a diffuse phase transformation. Figure 19 shows the variation of specific heat with temperature of three compositions of formulation E. For formulations containing 1 and 2 mole % Nd_2O_3, a distinct latent heat peak was observed, whereas for the sample containing 3 mole% Nd_2O_3, the latent heat peak was diffuse. A similar behavior was reported by Borman and Frisberg [45] for (Ba, Sr)TiO_3 solid solution. They explained the behavior using Devonshire's theory [46, 47], and related the diffuse heat capacity peak to the gradual change in polarization by the relation

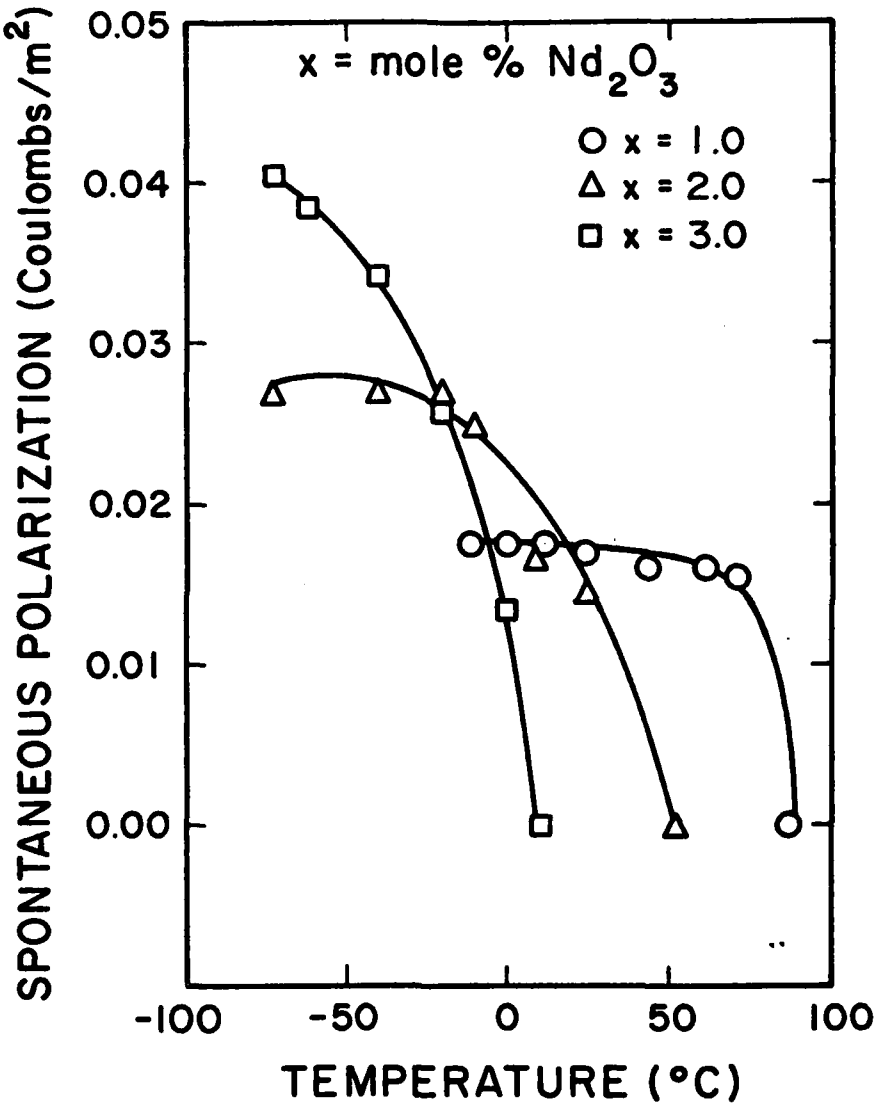

Figure 18. Variation of spontaneous polarization of formulation E with temperature.

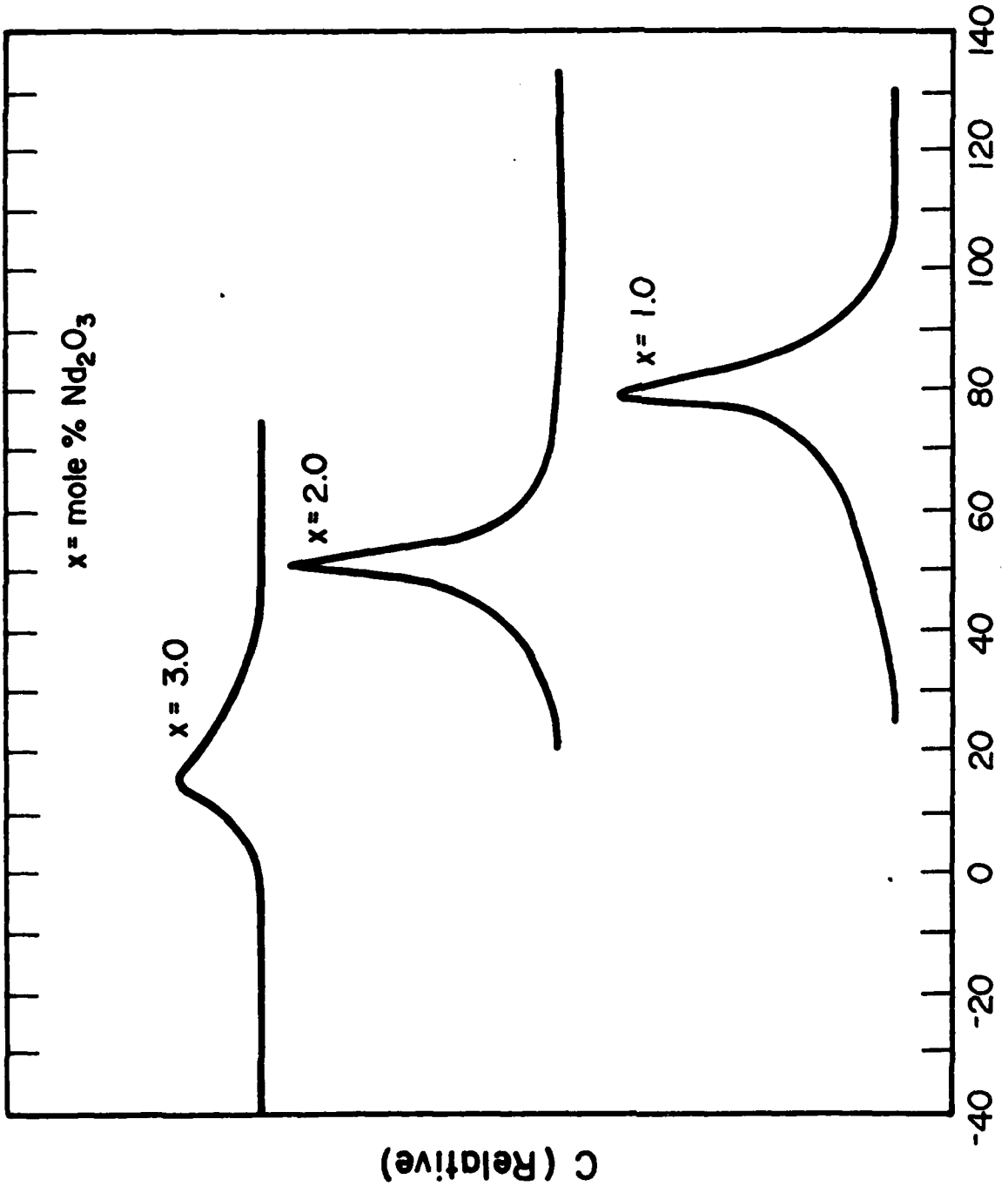

Figure 19. Variation of relative specific heat of formulation E with temperature.

$$\Delta C = \frac{1}{2C_w}\left(\frac{TdP_s}{dT}\right)^2 \qquad (13)$$

where C_w is the Curie Weiss Constant, P_s is the spontaneous polarization and ΔC is the height of the specific heat peak relative to the base line.

3.5 Summary

1. When Nd_2O_3 is added to $BaTiO_3$, the neodymium ions go in substitutionally on barium sites and charge compensation takes place by formation of titanium vacancies.

2. The solid solubility is greater than 10 mole % if the Nd_2O_3 is added as Nd_2O_3 . 3/2 TiO_2 in accordance with the defect structure.

3. Addition of neodymium oxide to barium titanate reduces the Curie temperature drastically; less than 3 mole % Nd_2O_3 shifts T_c below room temperature.

4. Nd_2O_3 doped $BaTiO_3$ has a very low dissipation factor above T_c, and the dissipation factor-temperature curve passes through a point of inflection at the Curie temperature.

5. The ferroelectric phase transformation becomes diffuse for doping levels of 3 mole % Nd_2O_3 and higher.

4. FILM FORMATION STUDIES

The graduate student working on this phase of the project left to take a job with Ferro Corporation in September, 1984, and his replacement did not complete his MS thesis with another professor until April, 1985. Therefore, studies on film formation were active for only half of the contract year and the results are presented in summary form. The necessary groundwork has been laid, and directions for research in the next contract year determined.

The metallo-organic compounds used in the $BaTiO_3$ film formation study were characterized by thermogravimetric analysis, NMR spectroscopy and IR spectroscopy. The titanium dimethoxy dineodecanoate and the barium neodecanoate were found to have almost the same temperature ranges of decomposition and peak decomposition temperatures. This is advantageous since the decomposition products of the two compounds would be formed at almost the same time and thus there would be minimum segregation of these, which should be reflected as a more uniform final fired product, $BaTiO_3$. Silver neodecanoate was found to have a peak decomposition temperature much lower than that of titanium dimethoxy dineodecanoate and barium neodecanoate, making it an attractive choice as an electrode material, especially for cofiring with the dielectric film. The NMR and IR spectroscopic analyses helped ensure that various batches of the compounds were the same, thus providing a means for identifying the compounds and for partial establishment of their structure by identification of their functional groups.

The films were deposited by spinning a solution of metallo-organic compounds onto silicon substrates. A range of concentrations of a 1:1 molar solution in xylene of titanium dimethoxy dineodecanoate and barium

neodecanoate which gave the most uniform wet films was identified. A different set of spinning parameters was established for the silver neodecanoate solution in xylene which gave uniform wet films for the chosen concentration of the solution.

The fired films of $BaTiO_3$ formed under these conditions were found to have a uniform thickness not exceeding a variation of 9% along a diameter. The SEM analysis of the surface structures at various points on the wafer indicated that there are no variation in surface structure due to this thickness variation. The fired films were concluded to be uniform.

The changes taking place in the films when they were heated was studied using optical hot stage microscopy. The study underlined the importance of the solvent evaporation stage in film formation. It also proved that the choice of the silicon wafer substrates was well made. The processes taking place at higher temperatures could not be studied since the resolution of the microscope was insufficient.

Weight loss studies during solvent evaporation demonstrated that it was not possible to remove the solvent completely in a reasonable time by drying at a temperature below the boiling point of the solvent. The studies also showed that the extent of the solvent removal was the same at different heating rates for the same drying temperature. The results indicated that there was an attractive interaction between the metallo-organic compounds and the solvent, which was a function of temperature.

From SEM studies on films dried at various heating rates and at various drying temperatures, it was concluded that a heating rate of

5°C/min, a drying temperature of 135°C and a drying time of 30 min. would result in a uniform dried film. The formation of a uniform dried film was important because any non-uniformity would be reflected in the fired films. The solvent removal in films was easier because of the partial evaporation of the solvent during spinning of the wet film onto the substrate.

The solvent evaporation studies revealed one of the problems of the MOD process: segregation. The segregation was revealed by electron diffraction of various regions of a film fired to 625°C. Certain regions showed the presence of TiO_2 while others showed the presence of $BaTiO_3$. Since segregation is favored by low heating rates where the chances of obtaining a uniform film are higher, a compromise has to be found which results in a heating rate that is not too high to cause rupture of the film and not too low to cause segregation. If that is not possible, then alternatives have to be found: a different solvent in which the solubilities of the metallo-organic compounds are almost the same; a different method of forming the wet film which would remove most of the solvent without causing segregation; or others.

The thermogravimetric analysis of a 1:1 molar solution in xylene of barium neodecanoate and titanium dimethoxy dineodecanoate indicated that the formation of $BaTiO_3$ occurred in the temperature range of 625-650°C, as discussed in Section 2. SEM analysis of a film fired at the rate of 5°C/min. showed crystalline $BaTiO_3$ in the matrix at 700°C which was absent at 600°C. The $BaTiO_3$ regions grew to form a uniform film at higher temperatures.

Electron diffraction studies of films fired to temperatures of 550° to 675°C showed $BaTiO_3$ forming from TiO_2 and $BaCO_3$. Regions that were completely $BaTiO_3$ were present at temperatures as low as 575°C, indicating the possibility of higher reaction rates in thin films as compared to reaction rates in bulk. If segregation, which might be the cause for the presence of TiO_2 at temperatures of 675°C, is totally removed, then there exists the exciting possibility of forming $BaTiO_3$ in films, at temperatures as low as 575°C.

Electron diffraction studies also revealed another type of non-uniformity in the films: either differing grain sizes at different parts of the film or differing degrees of preferred orientation at different parts of the film. The effect of these variations would be reflected as variations in electrical properties at various regions of the film.

Studies were made on suitable electrode materials and the means of forming electrode films. Since the studies on films established that $BaTiO_3$ forms below 700°C, silver entered the realm of possible electrode materials. The feasibility of producing Ag electrode films by the MOD process was explored, and adherent films of Ag were made. However, more studies have to be made to optimize firing conditions to obtain an adherent film of sufficient smoothness.

Electrical measurements were made at various points on some single layer films (~0.15 μm) that appeared smooth by SEM analysis, but the resistance of the films was too low to measure dielectric properties. It is not known whether this result was due to electrical shorts due to improper film formation (cracks, pores etc.) or due to dielectric break-

down during the process of measuring. When thicker films are made, it will be possible to make electrical measurements since there would be sufficient material to prevent dielectric breakdown. Studies are under way to produce thicker layers of dielectric films by either building thicker wet films and then firing to get a thicker fired film or by successive print and fire techniques.

REFERENCES

1. G. M. Vest and R. W. Vest, "A Generic Gold Conductor from Metallo-Organic Compounds", Int. J. Hybrid Microelectronics, 5[2], 62-68 (1982).

2. R. W. Vest, "Metallo-Organic Materials for Improved Thick Film Reliability", Final Technical Report, Purdue University, W. Lafayette, IN 47907, Contract No. N00163-79-C-0352 (1980).

3. G. M. Vest and R. W. Vest, "MOD Silver Metallization for Photovoltaics," Quarterly Technical Report, Purdue University, W. Lafayette, IN 47907, Contract No. DOE/JPL-956679-84/1 (1984).

4. R. W. Vest et al., "Ink Jet Printing of Hybrid Circuits", Int. J. Hybrid Microelectronics, 6[1] 261-267 (1983).

5. R. W. Vest and G. M. Vest, "Metallo-Organic Materials for Improved Thick Film Reliability", Final Technical Report, Purdue University, West Lafayette, IN. 47907, Contract No. N00163-83-C-0167 (1985).

6. S. F. Hulbert, "Models for Solid-State Reactions in Powdered Compacts: A review",J. Br. Ceram. Soc., 6[1], 11-19 (1969).

7. A. Amin et al., "Reaction of Anatase and Rutile with Barium Carbonate", J. Amer. Ceram. Soc., 66 [10] 733-738 (1983).

8. J. Kubo and K. Shinriki, "Chemical Reactions in Solid State:III, Reaction between $BaCO_3$ and TiO_2 in Solid State", J. Chem. Soc. Japan, Ind. Chem. Sect., 55[2], 49-51 (1952).

9. W. Trzebiatowski et al., "Mechanism of Synthesis of $BaTiO_3$", Roczniki Chem., 26[1], 12-33 (1952).

0. L. K. Templeton and J. A. Pask, " Formation of $BaTiO_3$ from $BaCO_3$ and TiO_2 in Air and in CO_2", J. Am. Ceram. Soc., 42[5] 212-216 (1959).

1. G. V. Bois et al., "Reactions in Mixtures of $BaCO_3$ and TiO_2 in Solid Form", Izv. Akad Nauk SSSR, Neorg. Materials, 10[4]658-660(1974).

2. R. E. Carter, "Kinetic Model for Solid-State Reactions", J. Chem. Phys., 34[6] 2010-2015 (1960).

3. J. Askill, "Tracer Diffusion Data for Metals, Alloys and Simple Oxides", pp 77-81, IFI/Plenum, New York (1970).

4. D. A. Venkatu and L. E. Poteat, "Diffusion of Ti in Single Crystal TiO_2", Material Sci. Eng., 5[5] 258-62 (1970).

5. T. S. Lundy and W. A. Coghlan, "Cation Self Diffusion in Rutile", J. Phys. Colloq., 34[9] 299-302 (1973).

6. K. Kitazawa et al., "Determination of Mass Transport Mechanism of Rutile by Sinusoidal Profile Decay Method", J. Am. Ceram. Soc., 60[7-8] 363-366 (1977).

7. F. H. Wohlbier, "Diffusion Defect Data vol. 20", pp 184-186, edited by F. H. Wohlbier, Trans. Technical Publication, Rockport Mass. 01966 (1979).

18. H. A. Sauer and S. S. Flaschen, "Positive Temperature Coefficient of Resistance Thermistor Materials for Electronic Applications", pp 41-46 in Proc. Electron. Components Symp., 7 th, Washington D. C., May 1956.

19. G. G. Herman, "Electrical Properties of $BaTiO_3$ Containing Samarium", Phys. Rev., 106[6], 1358-1359 (1957).

20. G. A. Smolenskii et al., "Ferroelectric Substitutional-Defect Solid Solution", Sov. Phys. Solid state, 1[10] 1573-1582 (1959).

21. O. Saburi, "Properties of Semiconductive Barium Titanate", J. Phys. Soc. Japan, 14[9] 1159-1174 (1959).

22. G. N. Tekster-Proskuryakova and I. T. Sheftel, "Semiconducting Barium and Strontium Titanates with Positive Temperature Coefficients of Resistivity", Sov. Phys. Solid State, 5[12] 2542-2548 (1963).

23. J. B. MacChesney et al., "Stabilized Barium Titanate Ceramic for Capacitor Dielectric", J. Am. Ceram. Soc., 46[5] 197-202 (1963).

24. R. Wernicke, "Influence of Kinetic Processes on the Electrical Conductivity", Phys. Stat. Sol. (a), 47[1], 139-143 (1978).

25. N. H. Chan and D. M. Smyth, "Defect Chemistry of Donor-Doped $BaTiO_3$", J. Am. Ceram. Soc., 67[4] 285-288 (1984).

26. K. S. Mazdiyasni and L. M. Brown, "Microstructure and Electrical Properties of Sc_2O_3-Doped, Rare Earth Oxide Doped and Undoped $BaTiO_3$", J. Am. Ceram. Soc., 54[11] 539-543 (1971).

27. T. Vojnovich and T. D. McGee, "Determination of Donor Gradients within Surface Barriers Formed on Dense Gd-Doped Barium Titanate", J. Am. Ceram. Soc., 52[7] 386-391 (1969).

28. T Ikeda and A. Watanabe, "Substituting Sites of Rare Earth Ions in $BaTiO_3$" Japan J. Appl. Phys., 7[3] 232-235 (1968).

29. K. Keizer and Burggraaf, "The Ferroelectric Phase Transition of Rare Earth Oxide Substituted Lead Titanate Ceramics", Ferroelectrics, 14[1/2], 671-673(1976).

30. D. Hennings and Goetz Rosenstein, "X-ray Structure Investigation of Lanthanum Modified Lead Titanate with A and B-Site Vacancies", Mat. Res. Bull., 7[12], 1505-1514(1972).

31. D. Hennings, "The Range of Existance of Perovskite Phase in the System $PbO-TiO_2-La_2O_3$", Mat. Res. Bull., 6[5], 329-340(1970).

32. N. G. Error and U. Balachandran, "Self Compensation in Lanthanum-Doped Strontium Titanate", J. Solid State Chem., 40[1], 85-91 (1981).

33. G. H. Jonker and E. E. Havinga, "The influence of Foreign Ions On The Crystal Lattice of Barium Titanate", Mat. Res. Bull., 17[3] 345-350 (1982).

34. G. V. Lewis and C. R. A. Catlow, "Computer Modelling of Barium Titanate", Radiation Effects, 73[1/4], 307-314 (1983).

35. H. Diamant et al., "Bridge for Accurate Measurement of Ferroelectric Hysteresis", The Review of Scientific Instruments, 28[1] 30-33

(1957).

36. D. E. Williams, "LCR-2, A Fortran Lattice Constant Refinement Program", United States Atomic energy Commission Research and Development Report IS-1052 (1964).

37. D. Kolar et al., "The $Nd_2O_3.4TiO_2$ Phase in the System Nd_2O_3-TiO_2, J. Less Common Metals, 60[1], 137-141 (1978).

38. D. Kolar et al., "Ceramic and Dielectric Properties of Selected Compositions in BaO-TiO_2-Nd_2O_3 System", Ber. Dt. Keram Ges., 55[7] 346-348 (1978).

39. D. Kolar et al., "Synthesis and Crystal Chemistry of $BaNd_2Ti_3O_{10}$, $BaNd_2Ti_5O_{14}$ and $Nd_4Ti_9O_{24}$", J. Solid State Chem., 38[2], 158 (1981).

40. W. J. Merz, Phys. Rev., "Double Hysteresis Loop of $BaTiO_3$ at the Curie Point", 91[3] 513-517 (1953).

41. G. Godefroy et al., "Diffuse Phase Transition in Co-doped Barium Titanate", Ferroelectrics, 34[4], 169-174 (1981).

42. S. Kuroda and K. Kubota, "Diffuse Phase Transitions in Rare Earth Ion Doped SBN", J. Phys. Chem. Solids, 42[7] 573-577 (1981).

43. N. Setter and L. E. Cross, "The Role of B-site Cation Disorder in Diffuse Transition Behavior of Perovskite Ferroelectrics", J. Appl. Phys., 51(8) 4356-4360 (1980).

44. A. P. Lavaynuk and A. S. Sigov, "Effect of Defect on the Properties

of Ferroelectrics and Related Materials Near the Point Corresponding to a Phase Transition of Second Kind", Izv. Akad. Nauk SSSR Ser. Fiz., 45[9] 1640-1645 (1981).

45. K. Ya. Borman and V. Ya. Frisberg, "Temperature and Concentration Dependence of the Specific Heat of (Ba, Sr)TiO_3 Solid Solution", Izv. Akad. Nauk SSSR Ser. Fiz., 39[6] 1336-1339 (1975).

46. A. F. Devonshire, "Theory of Barium Titanate", Phil. Mag., 40[309] 1040-1063 (1949).

47. A. F. Devonshire, "Theory of Barium Titanate", Phil. Mag., 42[333] 1065-1079 (1951).

END

FILMED

7-85

DTIC